UNIVERSIDADE DO VALE DO RIO DOS SINOS - UNISINOS
UNIDADE ACADÊMICA DE PESQUISA E PÓS-GRADUAÇÃO
PROGRAMA DE PÓS-GRADUAÇÃO EM GEOLOGIA
NÍVEL MESTRADO

TAMIRES NUNES ZARDIN

ASSESSING THE SIGNIFICANCE OF IDENTIFYING *GLOBIGERINOIDES RUBER ALBUS* MORPHOTYPES IN THE SOUTH ATLANTIC SUBTROPICAL GYRE DURING THE LATE PLEISTOCENE

São Leopoldo
2022

Tamires Nunes Zardin

ASSESSING THE SIGNIFICANCE OF IDENTIFYING *GLOBIGERINOIDES RUBER ALBUS* MORPHOTYPES IN THE SOUTH ATLANTIC SUBTROPICAL GYRE DURING THE LATE PLEISTOCENE

Dissertação apresentada como requisito parcial para obtenção do título de Mestre em Geologia sedimentar, pelo Programa de Pós-Graduação em Geologia da Universidade do Vale do Rio dos Sinos (UNISINOS).

Orientador(a): Prof. Dr. Karlos G. Diemer Kochhann

São Leopoldo

2022

Z36a Zardin, Tamires Nunes.

Assessing the significance of identifying *Globigerinoides ruber albus* morphotypes in the South atlantic subtropical gyre during the late pleistocene / Tamires Nunes Zardin. – 2022.

44 f. : il. ; 30 cm.

Dissertação (mestrado) – Universidade do Vale do Rio dos Sinos, Programa de Pós-Graduação em Geologia, 2022.

“Orientador: Prof. Dr. Karlos G. Diemer Kochhann”

Dados Internacionais de Catalogação na Publicação (CIP)

(Bibliotecária: Silvana Dornelles Studzinski – CRB 10/2524)

AGRADECIMENTOS

O presente trabalho foi realizado com apoio do Conselho Nacional de Desenvolvimento Científico e Tecnológico (CNPq), código de financiamento 430253/2018-4, projeto de pesquisa denominado *Mudanças paleoclimáticas durante o Mioceno tardio ao Plioceno: o Atlântico Sul no contexto paleoceanográfico global*, sob coordenação do Prof. Dr. Gerson Fauth.

RESUMO

Globigerinoides ruber albus é uma espécie de foraminífero planctônico onipresente em águas oceânicas superficiais tropicais e subtropicais. No entanto, sua taxonomia ainda é objeto de debate. Aqui, identificamos a nível de morfotipo um total de 1.816 espécimes de *G. ruber albus*, recuperados do estágio isotópico marinho (MIS) 14 a 9 no Site 517 do *Deep Sea Drilling Project* (DSDP), localizado no giro subtropical do Atlântico Sul. Os espécimes de *G. ruber* foram taxonomicamente divididos em sete morfotipos (cyclostoma, normal, platys, kummerform, elongatus cf. 1, elongatus pyramidical e twin) e sete parâmetros morfométricos foram medidos. Os morfotipos cyclostoma, normal, platys e kummerform apresentam diferenças significativas nas medidas morfométricas e nas proporções das medidas individuais, ocupando segmentos separados no morfoespaço. Também demonstramos que os caracteres morfológicos mais relevantes para a classificação dos morfotipos de *G. ruber albus* são altura e largura da última câmara e altura e largura da abertura. As análises dos isótopos estáveis de oxigênio ($\delta^{18}O$) e carbono ($\delta^{13}C$) mostraram que o morfotipo cyclostoma apresentou os valores de $\delta^{18}O$ mais altos e os valores de $\delta^{13}C$ mais baixos, indicando uma preferência por águas relativamente profundas e frias com baixa atividade simbionte. O morfotipo normal apresentou a assinatura de $\delta^{18}O$ mais baixa, evidenciando sua preferência por águas rasas e quentes, porém seus valores de $\delta^{13}C$ foram inferiores aos de platys e kummerform, sugerindo também redução da atividade do fotossimbionte. Considerando as mudanças nas abundâncias relativas, o morfotipo cyclostoma foi mais abundante durante os períodos interglaciais, enquanto o morfotipo kummerform foi mais abundante durante os períodos glaciais no giro subtropical do Atlântico Sul. Devido às diferenças morfométricas e isotópicas entre os morfotipos identificados aqui, sugerimos fortemente que futuros estudos paleoceanográficos considerem a identificação dos morfotipos cyclostoma, normal, platys e kummerform.

Palavras-chave: Foraminífero planctônico; morfometria; $\delta^{18}O$; $\delta^{13}C$; Quaternário

ABSTRACT

Globigerinoides ruber albus is a planktonic foraminiferal species widespread in tropical and subtropical surface ocean waters. Nevertheless, its taxonomy is still subject of debate. Here we classified at the morphotype level a total of 1816 *G. ruber albus* specimens recovered from marine isotopic stage (MIS) 14 to 9 at Deep Sea Drilling Project (DSDP) Site 517, located in the South Atlantic subtropical gyre. The specimens were taxonomically divided into seven morphotypes of *G. ruber* (cyclostoma, normal, platys, kummerform, elongatus cf. 1, elongatus pyramidical and twin) and seven morphometric parameters were measured. The morphotypes *G. ruber albus* cyclostoma, *G. ruber albus* normal, *G. ruber albus* platys and *G. ruber albus* kummerform present significant differences of morphometric measurements, as well as of ratios between individual measurements, occupying separate segments of morphospace. We also demonstrate that the most relevant morphological characters for the classification of *G. ruber albus* morphotypes are height and width of the last chamber, and height and width of the aperture. Stable oxygen ($\delta^{18}O$) and carbon ($\delta^{13}C$) isotope analyses showed that the *G. ruber albus* cyclostoma morphotype presented the highest $\delta^{18}O$ values and the lowest $\delta^{13}C$ values, indicating a preference for relatively deep and cold waters with low symbiont activity. The *G. ruber albus* normal morphotype showed the lowest $\delta^{18}O$ signature, evidencing its preference for shallow and warm waters, however its $\delta^{13}C$ values were lower than those of *G. ruber albus* platys and *G. ruber albus* kummerform, also suggesting reduced photosymbiont activity. Considering changes in relative abundances, although minor, the *G. ruber albus* cyclostoma morphotype was more abundant during interglacial periods, whereas the *G. ruber albus* kummerform morphotype was more abundant during glacials in the South Atlantic subtropical gyre. Due to the morphometric and isotopic differences between the morphotypes identified here, we suggest that future paleoceanographic studies consider identifying the *G. ruber albus* cyclostoma, *G. ruber albus* normal, *G. ruber albus* platys and *G. ruber albus* kummerform morphotypes.

Key-words: Planktonic foraminifera; morphometry; $\delta^{18}O$; $\delta^{13}C$; Quaternary

SUMÁRIO

1 INTRODUÇÃO

Os foraminíferos planctônicos são organismos unicelulares, pertencentes ao reino protista, extremamente abundantes em ambientes marinhos. Sua abundância e ótima preservação das testas em sedimentos oceânicos produz um dos mais completos registros fósseis da Terra (Boltovskoy, 1965; Kucera, 2007). Por serem altamente sensíveis a variações ambientais, os foraminíferos planctônicos são um instrumento essencial para reconstruções paleoceanográficas e estudos bioestratigráficos (Ericson & Wollin, 1968; Hutson, 1980; Katz et al., 2010). Dentre os foraminíferos planctônicos quaternários, *Globigerinoides ruber* é uma das espécies mais usadas em estudos paleoceanográficos de regiões tropicais e subtropicais (Wang, 2000; Kuroyanagi & Kawahata, 2004; Lin et al., 2004; Kawahata, 2005; Löwemark et al., 2005; Steinke et al., 2005), principalmente em estudos de paleotemperatura superficial oceânica (LoDico et al, 2006; Sadekov et al, 2008; Ganssen et al, 2010; Weldeab et al., 2014), pois habita massas d'água superficiais, é portadora de simbiontes dinoflagelados (Bé et al., 1977; Hemleben et al., 1989; Schiebel & Hemleben 2017) e pode ser abundante tanto em regiões de ressurgência, que apresentam condições eutróficas, quanto em giros subtropicais, que apresentam condições oligotróficas (Kemle-von-Mücke & Hemleben 1999; Schiebel et al., 2004).

A taxonomia e a divisão entre os morfotipos de *G. ruber albus* tem sido objeto de revisões e inúmeros debates nos últimos tempos, assim como seu significado ecológico (Numberger et al., 2009; Aurahs et al., 2011; Bonfardeci et al. 2018; Morard et al., 2019). Neste trabalho, é nosso objetivo avaliar: (1) se a classificação dos morfotipos de *G. ruber albus* como s.s. e s.l. é suficiente para estudos paleoambientais, (2) se as diferenças entre os morfotipos definidos visualmente são morfometricamente significativas e (3) se havia diferentes preferências paleoecológicas entre os morfotipos de *G. ruber albus* entre os estágios glacial e interglacial (MIS 9 a MIS 14) no giro subtropical do Atlântico Sul. As características de cada morfotipo são descritas nos próximos capítulos.

O manuscrito do artigo desta dissertação de mestrado está formatado de acordo com as normas do periódico *Journal of Foraminiferal Research*, classificado no estrato Qualis – CAPES como B1, ao qual foi submetido.

2 GLOBIGERINOIDES RUBER

Devido à coloração avermelhada das carapaças encontradas, d'Orbigny (1839) classificou a espécie inicialmente como *Globigerina rubra*. O fenótipo alba foi definido por Cushman (1914) à mesma espécie. Posteriormente, Cushman (1927) incluiu *Globigerina rubra* ao novo gênero *Globigerinoides* devido à presença de aberturas suplementares.

Globigerinoides ruber (d'Orbigny, 1839) é uma espécie com o enrolamento trocoespiral médio a alto, com três câmaras subesféricas no último verticilo na fase adulta, que aumentam de tamanho de forma moderada. Apresentam suturas radiais, superfície grosseiramente perfurada, abertura primária umbilical larga em forma de arco, com duas aberturas secundárias do lado espiral (Kennett & Srinivasan, 1983; Schiebel & Hemleben, 2017).

Existem dois fenótipos (cromótipos) desta espécie: *G. ruber pink* e *G. ruber white*, sendo a *pink* extinta nos oceanos Índico e Pacífico há ~ 120 Ka e atualmente restrita ao oceano Atlântico e ao mar Mediterrâneo. A variedade *white* está presente em todas as bacias oceânicas (Thompson et al., 1979; Schiebel & Hemleben, 2017). Além das distintas distribuições geográficas, os cromótipos apresentam sinais isotópicos significativamente diferentes (Robbins & Healy-Williams, 1991; Rohling et al., 2004; Aze et al., 2011). Estudos baseados em dados genéticos moleculares recentes apoiam fortemente a separação dos dois cromótipos em espécies distintas (Aurahs et al., 2011; Morard et al., 2019). Morard et al. (2019) sugeriram essa separação em nível subespecífico, como *Globigerinoides ruber albus* para a variação branca.

A distribuição de *G. ruber albus* se estende ainda mais nas latitudes temperadas do Oceano Atlântico do que a variedade *pink,* que pode ser considerada uma espécie de verão, enquanto o fenótipo *albus* ocorre durante todo o ano (Kemle-von-Mücke & Hemleben, 1999). A espécie *G. ruber albus* se mostra muito adaptável em condições ecológicas variáveis quando comparado com outras espécies modernas do gênero *Globigerinoides.*

2.1 Morfotipos de *Globigerinoides ruber albus*

Vários morfotipos de *G. ruber albus* são reconhecidos na literatura e até mesmo classificados em nível de espécie. *Globigerinoides elongatus* (d'Orbigny, 1826), por exemplo, é caracterizada pela forma trocoespiral com enrolamento mais alto, com a última câmara achatada ou não; *Globigerinoides pyramidalis* (Van den Broeck, 1876) com enrolamento trocoespiral mais alto que *G. elongatus* e quatro câmaras no último verticilo e *Globigerinoides cyclostomus* (Galloway & Wissler, 1927) para formas com a testa compacta e abertura pequena e arredondada. Baseados na filogenia dos foraminíferos planctônicos cenozoicos, Kennett e Srinivasan (1983) sugeriram que estes morfotipos são variantes fenotípicas de uma mesma espécie: *Globigerinoides ruber*. Em estudos posteriores foram descritos vários morfotipos, geralmente identificados por códigos numéricos (Robbins & Healy-Williams, 1991; Löwemark et al., 2005; Sadekov et al., 2008).

Wang (2000), utilizando critérios taxonômicos, como formato das câmaras, lobação dos contornos da carapaça e forma/posição das aberturas, dividiu todos os morfotipos até então reconhecidos em dois grupos: *G. ruber* sensu stricto (s.s.) e *G. ruber* sensu lato (s.l.). O morfotipo *G. ruber* s.s. apresentam três câmaras esféricas no verticilo final e abertura primária larga, em forma de arco alto com duas aberturas secundárias. Os morfotipos anteriormente descritos como *Globigerinoides elongatus* (d'Orbigny, 1826), *Globigerinoides pyramidalis* (Van den Broeck, 1876) e *Globigerinoides cyclostomus* (Galloway & Wissler, 1927) foram agrupados como *G. ruber* s.l. Análises de isótopos estáveis feitas por Wang (2000) sugerem que os dois morfotipos habitam profundidades diferentes, com *G. ruber* s.s. vivendo nos primeiros 30 metros da coluna d'água enquanto *G. ruber* s.l. habita profundidades abaixo dos 30 metros.

Utilizando os mesmos critérios descritos por Wang (2000) para classificar os morfotipos de *G. ruber albus* em um estudo feito no Golfo do México, Thirumalai et al. (2014) refutaram a hipótese de que os diferentes morfotipos habitam profundidades diferentes no local de estudo. As análises geoquímicas não mostraram variações significativas entre os morfotipos.

Numberger et al. (2009) reconheceram quatro morfotipos no estudo de dois testemunhos do mar Mediterrâneo. O morfotipo denominado normal engloba os mesmos espécimes referidos como *G. ruber* s.s. por Wang (2000). O morfotipo

platys, caracterizado por espécimes com a última câmara compactada, achatada e assimétrica, com abertura relativamente pequena, pode ser parcialmente comparável com s.l. de Wang (2000). O terceiro morfotipo, denominado elongate, refere-se às formas correspondentes ao conceito da espécie *Globigerinoides pyramidalis* de Van den Broeck (1876) e ao s.l. de Wang (2000). Neste mesmo estudo, Numberger et al (2009) sugerem que o morfotipo platys é mais abundante durante os períodos glaciais, enquanto o elongate é mais abundante nas deglaciações e interglaciais, durante os MIS 2 a 1 e MIS 12 a 9. Além desses três, Numberger et al. (2009) descrevem o morfotipo denominado kummerform (referenciado pela primeira vez por Berger, 1969), relativo a formas em que a câmara final é significativamente menor que as câmaras anteriores, podendo ser esférica ou achatada. Hecht & Savin (1970) defendem a hipótese de que essa câmara final diminuta das formas kummerforms é uma resposta ao estresse ambiental causado pelo resfriamento da coluna d'água, com as análises isotópicas apontando temperaturas oceânicas superficiais entre 1° e 4,5 °C mais frias do que os valores estimados para o morfotipo normal.

O morfotipo twin foi caracterizado pela primeira vez por Kontakiotis et al. (2017) e refere-se a espécimes com duas últimas câmaras simétricas e, consequentemente, duas aberturas principais.

Bonfardeci et al. (2018), no estudo de um testemunho coletado no Atlântico Norte, analisaram a distribuição de seis morfotipos da espécie *G. ruber* ao longo dos períodos glaciais e interglaciais dos últimos 74,7 Ka, sendo eles s.s. (Wang, 2000); kummerform (Numberger et al., 2009); *G. elongatus* que é equivalente ao morfotipo platys de Numberger et al (2009); *G. elongatus* cf.1 corresponde parcialmente ao morfotipo elongate de Numberger et al. (2009) e sendo uma possível variante morfológica dentro da descrição da espécie *Globigerinoides elongatus* (d'Orbigny, 1826); *G. elongatus* pyramidical, que tem as características da espécie *Globigerinoides pyramidalis* descrita por Van den Broeck (1876) e um sexto morfotipo denominado cyclostoma, que é consistente com a descrição morfológica da espécie *Globigerina cyclostoma* de Galloway e Wissler (1927). De acordo com Bonfardeci et al. (2018), o morfotipo cyclostoma é o menos estudado, até o momento não foram publicados dados genéticos moleculares para confirmar se o mesmo é uma espécie diferente, conforme proposto por Galloway e Wissler (1927), logo, segue sendo classificada como um morfotipo de *G. ruber albus*. As análises

micropaleontológicas e geoquímicas de Bonfardeci et al. (2018) indicam algumas preferências ecológicas dos morfotipos, com cyclostoma atingindo suas abundâncias máximas durante os períodos glaciais e *G. elongatus* nos interglaciais.

No presente trabalho classificamos os espécimes de *G. ruber albus,* considerando o máximo de morfotipos descritos na literatura, entre os sete morfotipos a seguir: normal, platys, e kummerform seguindo os critérios de Numberger et al. (2009), twin de Kontakiotis et al. (2017), cyclostoma, elongatus cf.1 e elongatus pyramidical de Bonfardeci et al. (2018).

Gmail **Tamires nunes zardin <tamireszardin@gmail.com>**

Submission of Manuscript Zardin et al

1 ensagem

Tamires nunes zardin <tamireszardin@gmail.com> 23 de fevere ro de 2022 22:49
Para: JFReditorinchief@gmail.com

Dear Editor,

Please find attached all files related to the submission of the manuscript entitled "Assessing the significance of identifying *Globigerinoides ruber albus* morphotypes in the South Atlantic subtropical gyre during the late Pleistocene" to the Journal of Foraminiferal Research. Additional information on the submission is provided in the cover letter file.

I would be grateful if you could confirm receiving the files.

Looking forward to hearing from you.

Sincerely,

Tamires Nunes Zardin
Graduada em Ciências Biológicas
Mestranda em Geologia sedimentar
Paleontologia aplicada
Instituto Tecnológico de Paleoceanografia e Mudanças Climáticas - itt **OCEAN**EON
F: 55- 51 98212-3513

12 anexos

- **Cover Letter_Zardin_et_al.pdf** 70K
- **Supplementary material Zardin_et_al.pdf** 337K
- **Zardin_et_al_.docx** 124K
- **Zardin_et_al.pdf** 1196K
- **Sup Table Stable isotope morphotypes Zardin et al.xlsx** 6K
- **Sup Table morphometric all specimens Zardin et al.xlsx** 145K
- **Figure_3_Zardin_et_al.pdf** 155K
- **Figure_4_Zardin_et_al.pdf** 1049K
- **Figure_6_Zardin_et_al.pdf** 149K
- **Figure_2_Zardin_et_al.pdf** 5176K
- **Figure_1_Zardin_et_al.pdf** 1546K
- **Figure_5_Zardin_et_al.pdf** 6593K

3 ARTIGO

RRH: *G. RUBER ALBUS* MORPHOTYPES SIGNIFICANCE

LRH: ZARDIN AND OTHERS

ASSESSING THE SIGNIFICANCE OF IDENTIFYING *GLOBIGERINOIDES RUBER ALBUS* MORPHOTYPES IN THE SOUTH ATLANTIC SUBTROPICAL GYRE DURING THE LATE PLEISTOCENE

TAMIRES NUNES ZARDIN [1,2], KARLOS G. DIEMER KOCHHANN [1,2], JORGE VILLEGAS. MARTÍN [1], GUILHERME KRAHL [1,2], GERSON FAUTH [1,2]

[1] Technological Institute for Paleoceanography and Climate Change (itt OCEANEON), UNISINOS University, São Leopoldo, Brazil

[2] Geology Graduate Program, UNISINOS University, São Leopoldo, Brazil

Mailing address: Av. Unisinos, 950, C11, CEP: 93022-750, São Leopoldo, RS, Brazil
E-mail: tamireszardin@gmail.com

Abstract: *Globigerinoides ruber albus* is a planktonic foraminiferal species widespread in tropical and subtropical surface ocean waters. Nevertheless, its taxonomy is still subject of debate. Here we classified at the morphotype level a total of 1816 *G. ruber albus* specimens recovered from marine isotopic stage (MIS) 14 to 9 at Deep Sea Drilling Project (DSDP) Site 517, located in the South Atlantic subtropical gyre. The specimens were taxonomically divided into seven morphotypes of *G. ruber* (cyclostoma, normal, platys, kummerform, elongatus cf. 1, elongatus pyramidical and twin) and seven morphometric parameters were measured. The morphotypes *G. ruber albus* cyclostoma, *G. ruber albus* normal, *G. ruber albus* platys and *G. ruber albus* kummerform present significant differences of morphometric measurements, as well as of ratios between individual measurements, occupying separate segments of morphospace. We also demonstrate that the most relevant morphological characters for the classification of *G. ruber albus* morphotypes are height and width of the last chamber, and height and width of the aperture. Stable oxygen ($\delta^{18}O$) and carbon ($\delta^{13}C$) isotope analyses showed that the *G. ruber albus* cyclostoma morphotype presented the $\delta^{18}O$ highest values and the lowest $\delta^{13}C$ values, indicating a preference for relatively deep and cold waters with low symbiont activity. The *G. ruber albus* normal morphotype showed the lowest $\delta^{18}O$ signature, evidencing its preference for shallow and warm waters, however its $\delta^{13}C$ values were lower than those of *G. ruber albus* platys and *G. ruber albus* kummerform, also suggesting reduced photosymbiont activity. Considering changes in relative abundances, although minor, the *G. ruber albus* cyclostoma morphotype was more abundant during interglacial periods, whereas the *G. ruber albus* kummerform morphotype was more abundant during glacials in the South Atlantic subtropical gyre. Due to the morphometric and isotopic differences between the morphotypes identified here, we suggest that future paleoceanographic studies consider identifying the *G. ruber albus* cyclostoma, *G. ruber albus* normal, *G. ruber albus* platys and *G. ruber albus* kummerform morphotypes.

Key-words**:** Planktonic foraminifera; morphometry; $\delta^{18}O$; $\delta^{13}C$; Quaternary

1 INTRODUCTION

Planktonic foraminifera are unicellular protists, extremely abundant in marine environments, and have a high preservation potential in ocean sediments, characterizing one of the best fossil records on Earth (Boltovskoy, 1965; Kucera, 2007). Because they are highly sensitive to environmental variations, planktonic foraminifera are an essential tool for paleoceanographic reconstructions and biostratigraphic studies (e.g., Ericson & Wollin, 1968; Hutson, 1980; Katz et al., 2010). Among Quaternary planktonic foraminifera, *Globigerinoides ruber* (d'Orbigny, 1839) is one of the most used species in paleoceanographic studies of tropical and subtropical regions (e.g., Wang, 2000; Kuroyanagi & Kawahata, 2004; Lin et al., 2004; Kawahata, 2005; Löwemark et al., 2005; Steinke et al., 2005). *Globigerinoides ruber* inhabits surface waters and can be abundant both in eutrophic upwelling regions and in oligotrophic subtropical gyres (Kemle-von-Mücke & Hemleben 1999; Schiebel et al., 2004). There are two chromotypes of this species: *G. ruber* pink and *G. ruber* white. Recent studies based on genetic data support that the two chromotypes are, in fact, distinct species (Aurahs et al., 2011; Morard et al., 2019). Morard et al. (2019) proposed the subspecies *Globigerinoides ruber albus* for the white variant, being this the taxonomic definition adopted in our study.

Several morphotypes of *Globigerinoides ruber albus* are recognized in the literature and even classified at the species level, as is the case of *Globigerinoides elongatus* (d'Orbigny, 1826), *Globigerinoides pyramidalis* (Van den Broeck, 1876) and *Globigerinoides cyclostomus* (Galloway & Wissler, 1927). However, Kennett and Srinivasan (1983), based on the phylogeny of Cenozoic planktonic foraminifera, suggested that these previously described species are phenotypic variants of the same species: *Globigerinoides ruber.*

Wang (2000), using taxonomic criteria such as chambers shapes, lobation of test contours and shape/position of apertures, assigned all morphotypes recognized until then to two groups: *G. ruber* sensu stricto (s.s.) and *G. ruber* sensu lato (s.l.). The *G. ruber* s.s. presents three spherical chambers in the final whorl, a wide primary aperture in the form of a high arch, and two secondary apertures. The morphotypes previously described as *Globigerinoides elongatus* (d'Orbigny, 1826), *Globigerinoides pyramidalis* (Van den Broeck, 1876) and *Globigerinoides cyclostomus* (Galloway & Wissler, 1927) were grouped as *G. ruber* s.l. Wang (2000) attempted to subdivide *G. ruber* s.l. into two groups according to the

height of the spire, but due to similar stable carbon ($\delta^{13}C$) and oxygen ($\delta^{18}O$) isotope signatures regrouped these forms. Stable isotope analyses suggest that the two morphotypes inhabit different depths (Wang, 2000), with *G. ruber* s.s. living in the first 30 meters of the water column and *G. ruber* s.l. inhabiting depths below 30 meters.

Numberger et al. (2009), in their study of two cores in the Mediterranean Sea, divided *G. ruber* specimens into four morphotypes: normal (s.s. of Wang, 2000), platys, elongate (partially equivalent to s.l. of Wang, 2000) and kummerform (first described by Berger, 1969). In the Mediterranean Sea, these morphotypes presented relative abundance changes through glacial and interglacial cycles (Numberger et al., 2009). Subsequently, Kontakiotis et al. (2017) renamed the morphotypes as A, B and C (except for kummerform) and defined a new morphotype, named D or twin. Bonfardeci et al. (2018), in the study of a core collected in the North Atlantic, divided specimens into six morphotypes, being *G. ruber* s.s. (Wang, 2000), *G. ruber* kummerform and *G. ruber* cyclostoma, the latter being less studied so far, as well as morphotypes assigned to *Globigerinoides elongatus*, such as *Globigerinoides elongatus* cf. 1, *Globigerinoides elongatus* pyramidical. Even though the taxonomy and subdivision of *G. ruber albus* morphotypes have been the subject of revisions and debates, most paleoenvironmental studies classify *G. ruber albus* morphotypes as s.s. and s.l. (e.g., Kuroyanagi & Kawahata, 2004; Löwemark et al., 2005; Kuroyanagi et al., 2008; Thirumalai et al., 2014; Carter et al., 2017; Jayan et al., 2021).

Here we classified at morphotype level all specimens of *Globigerinoides ruber albus* recovered along Marine Isotope Stages (MIS) 14 to 9 (530 to 330 ka, late Pleistocene) at Deep Sea Drilling Project (DSDP) Site 517, located in the South Atlantic subtropical gyre. We considered the maximum number of morphotypes described in the literature, being those normal, platys, and kummerform following the criteria of Numberger et al. (2009), twin by Kontakiotis et al. (2017), and cyclostoma, *Globigerinoides elongatus* cf. 1 and *Globigerinoides elongatus* pyramidical by Bonfardeci et al. (2018). We will refer to *G. elongatus* morphotypes as elongatus cf. 1 and elongatus pyramidical, because several works approach the plexus elongatus as *G. ruber* morphotypes (e.g., Kuroyanagi & Kawahata, 2004; Löwemark et al., 2005; Carter et al., 2017; Jayan et al., 2021). A total of 1816 specimens were classified and measured, and we additionally ran $\delta^{18}O$ and $\delta^{13}C$ analyses of the four most abundant morphotypes for each MIS. We aim to assess: (1) whether the classification of *G. ruber albus* morphotypes as *G. ruber albus* s.s. and *G. ruber albus* s.l. is sufficient for paleoceanographic studies, (2) whether the differences between the visually defined morphotypes are morphometrically significant, and (3) whether there were different

paleoecological preferences among the *G. ruber albus* morphotypes between glacial and interglacial stages (MIS 9 to MIS 14) in the South Atlantic subtropical gyre.

2 MATERIALS AND METHODS

2.1 SITE LOCATION, SAMPLING STRATEGY AND AGE MODEL

Site 517 was drilled during Expedition 72 of DSDP, at a depth of 2963 meters, on the western flank of the Rio Grande rise, southwestern Atlantic Ocean (30°56.81'S; 38°02.47'W, figure 2). We sampled in 5-10 cm intervals the succession between Sections 517-2W-1 and 517-2W-2, spanning 2.89 to 5.46 meters below the seafloor (mbsf), and totaling 27 samples. Lithologically, this interval is composed of calcareous ooze (Pujol, 1983).

We constructed an age model for the studied interval of Site 517 by correlating the benthic foraminiferal $\delta^{18}O$ record of Grazzini et al. (1983) with the global stack LR04 of Lisiecki and Raymo (2005). The age model was constructed using the software QAnalySeries (Kotov & Pälike, 2018) and is presented in Supplementary Figure S1.

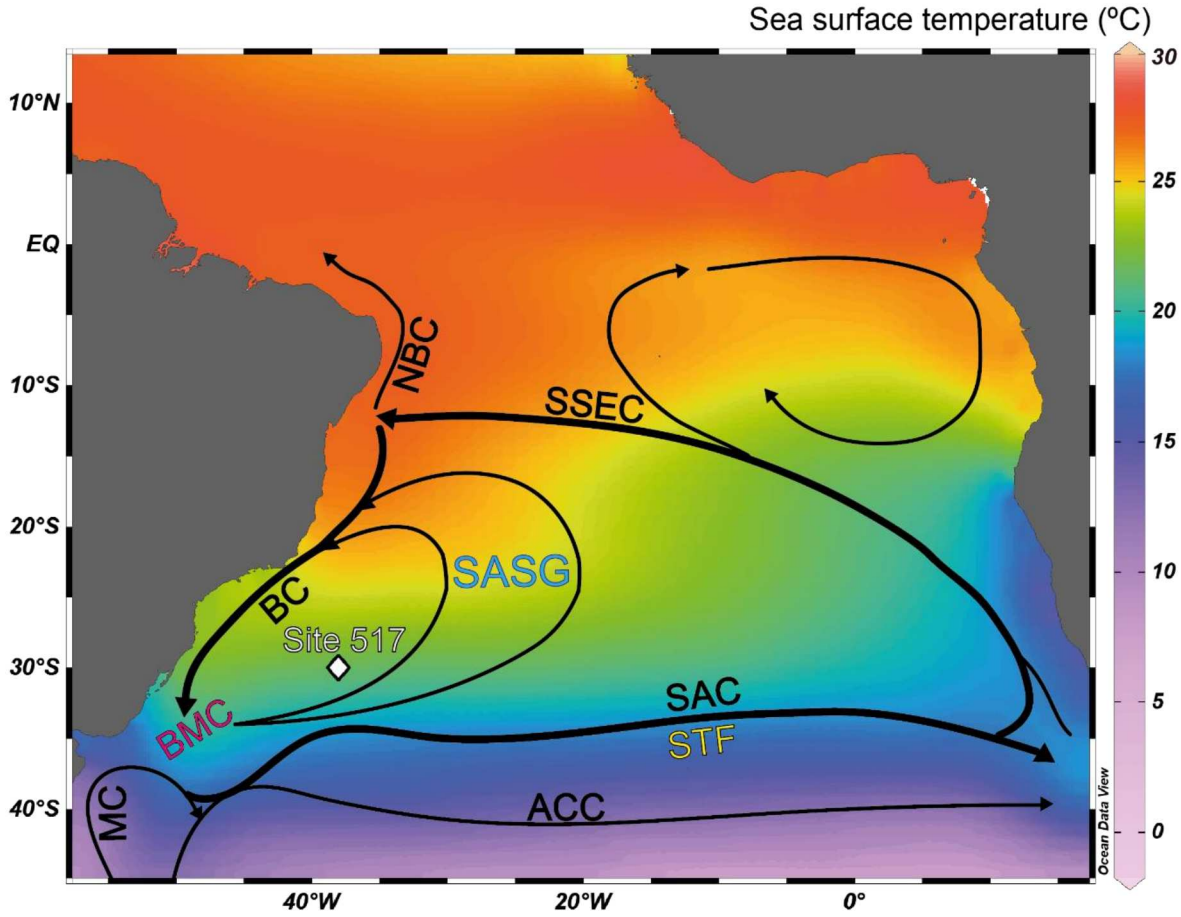

FIGURE 1- Location of site DSDP 517 (white diamond) in the South Atlantic subtropical gyre (SASG). Map showing mean annual surface temperature (Locarnini et al., 2019), and generated with the software Ocean Data View (Schlitzer, 2020). Schematic arrows represent main surface ocean currents in the South Atlantic (Stramma & England, 1999): Antarctic Circumpolar Current (ACC), Brazil Current (BC), Brazil-Malvinas Confluence (BMC), Malvinas Current (MC), North Brazil Current (NBC), South Atlantic Current (SAC), Southern South Equatorial Current (SSEC). STF: Subtropical Front.

2.2 SAMPLE PREPARATION AND PICKING

Sediment samples were prepared as follows: (1) Weighing dry samples (approximately 10 g of sediments per sample); (2) soaking samples in deionized water for 15 minutes; (3) washing in running water using 125 μm and 45 μm sieves; (4) drying residues in an oven at 40°C for at least 24 h.

Once dry, samples were split, when necessary, until between 300 and 600 planktonic foraminiferal specimens were present in the aliquots. We picked all planktonic foraminifera from the >125 μm aliquots to collect only adult specimens.

2.3 MORPHOTYPES IDENTIFICATION, IMAGE ACQUISITION AND MORPHOMETRIC MEASUREMENTS

The typical spiny wall texture was recognized in all morphotypes; therefore, identification was based on the following taxonomic criteria: (1) wall texture; (2) shape of the spire; (3) number and form of chambers in the last whorl; (4) shape, dimension, and position of the primary and secondary apertures. Based on these characteristics, we identified the morphotypes normal, platys, cyclostoma, kummerform, elongatus cf. 1, elongatus pyramidical and twin according to the literature (Numberger et al., 2009, Kontakiotis et al., 2017, Bonfardeci et al., 2018) (Figure 2). The *G. ruber albus* normal morphotype has three spherical chambers in the final whorl, a wide primary aperture in the form of a high arch, and two secondary apertures. *G. ruber albus* cyclostoma has the most compact arrangement of chambers, a rounded and small aperture in relation to the last chamber, and a thick test wall. Specimens assigned to the *G. ruber albus* platys morphotype present a flat and asymmetrical final chamber, with a relatively small aperture and a generally wider than tall test in apertural view. The *G. ruber albus* kummerform morphotype refers to specimens with the last chamber

significantly smaller than the previous ones, usually less than half of the size of the penultimate chamber; this last chamber can be flattened or round, as can be the aperture. Elongatus cf. 1 differs from platys by its higher spire, having or not a flattened last chamber. elongatus pyramidical is characterized by having a higher spire than elongatus cf.1 and by having four chambers in the last whorl. The twin morphotype refers to specimens with two last symmetrical chambers and, consequently, two main apertures.

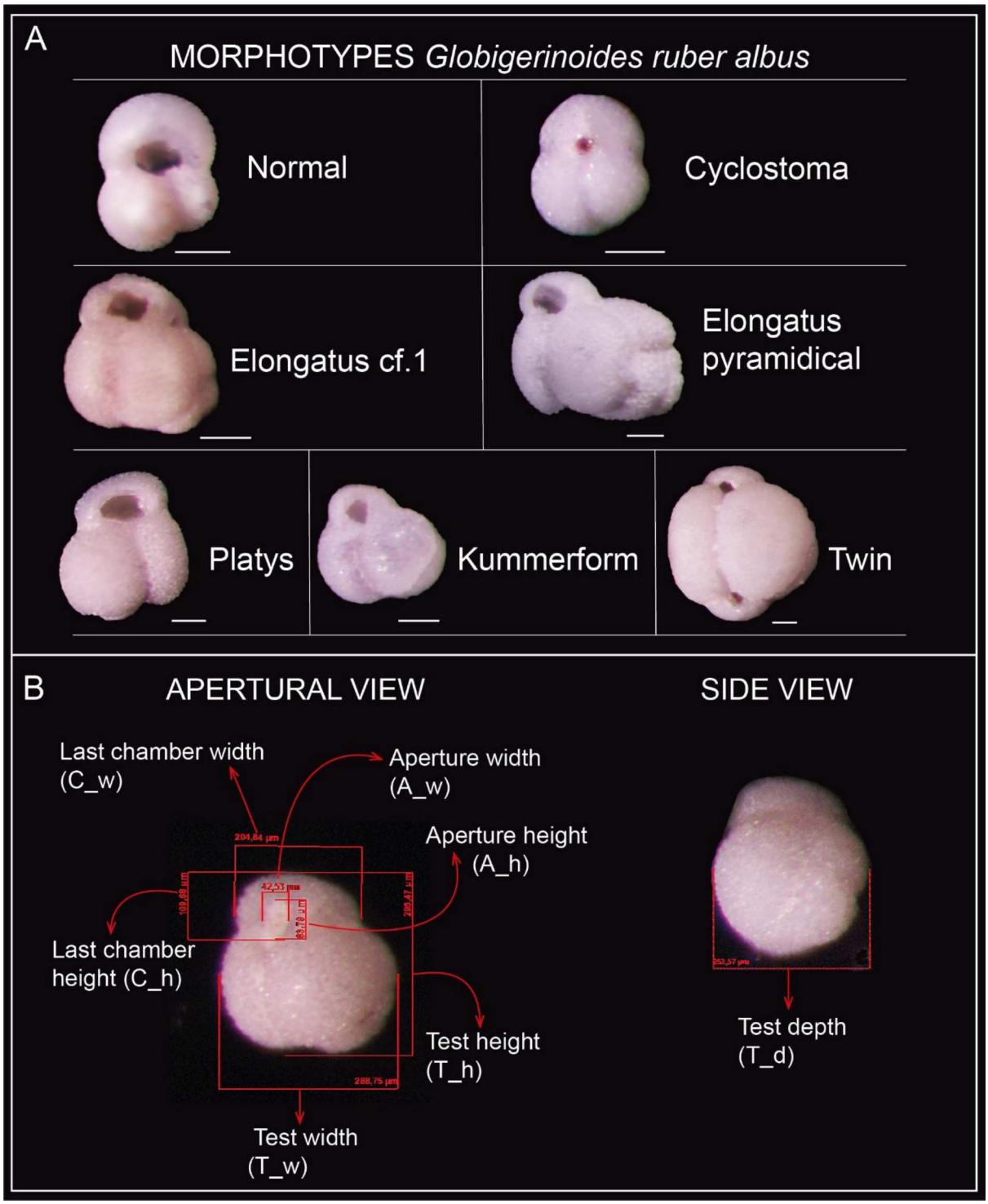

FIGURE 2-Optical micrographs of *G. ruber albus* from DSDP Site 517. A: Images of the seven recognized morphotypes. Scale bar of 100 μm. B: Identification of the seven morphometric parameters (and their abbreviations) measured for all *G. ruber albus* specimens

All specimens of *G. ruber albus* were imaged and manually measured with the software AxioVision connected to a Zeiss Discovery.V20 stereomicroscope, at the Technological Institute for Paleoceanography and Climate Change (itt OCEANEON). Specimens were imaged in standard apertural and side views.

A total of seven morphometric parameters were measured, namely: test (T) width (w), height (h) and depth (d), last chamber (C) width (w) and height (h), and aperture (A) width (w) and height (h) (Figure 2). We analyzed these parameters as: aperture height (A_h); aperture width (A_w); test height (T_h); test width (T_w); test depth (T_d); last chamber height (C_h); last chamber width (C_w); aperture height/width ratio (A_hw); last chamber height/width ratio (C_hw); ratio between the area of the last chamber and the area of the aperture (CA_a), test width/depth ratio (T_wd); test height/width ratio (T_hw); test height/depth ratio (T_hd).

2.4 STATISTICAL ANALYSIS

A classical cluster analysis was performed to identify similarities among the considered morphological parameters (aperture height, last chamber height, last chamber width, test height, test depth, and test width) for each one of the identified morphotypes. The UPGMA strategy (Unweighted Pair Group Method using Arithmetic Averages) and the Euclidean distance coefficient were used in the analysis. In addition, we ran the Mann-Whitney test to compare all morphometric parameters among all morphotypes. Although the twin morphotype presents low abundances throughout the studied interval at DSDP Site 517, we included it in the analysis, due to its remarkably different morphology. The software PAST – Paleontological Statistics (v. 3.15; Hammer et al., 2001) was used for statistical analyses, using a significance level of 5% for all tests.

2.5 STABLE ISOTOPE ANALYSIS

We measured the $\delta^{18}O$ and $\delta^{13}C$ signatures of the morphotypes normal, platys, cyclostoma and kummerform from six samples, each sample representing a marine isotopic

stage (MIS). Six specimens of each morphotype were placed in vials, covered with alcohol 95% and broken with a needle, aiming to expose the inner part of the chambers. They were then placed in an ultrasonic bath, for between 60 and 75 seconds, to release clay and possible contaminant phases. With a pipette, we collected the alcohol with suspended particles, and then were dried in an oven at ~38°C for at least 24 hours. After drying, samples were analyzed with an isotope ratio mass spectrometer Thermo Scientific MAT 253 (IRMS), coupled with a Thermo Scientific Kiel IV automatic carbonate preparation device at itt OCEANEON. Data were calibrated against the international standards IAEA 603 and IAEA CO-8, as well as the internal standard SPH2L (Crivellari et al., 2021). Reproducibility of the IAEA 603 standard over the measurement period was 0.05 for $\delta^{13}C$ and 0.08 for $\delta^{18}O$. All data are presented in parts per mil (‰) relative to Vienna Pee Dee Belemnite (VPDB).

4 RESULTS

4.1 MORPHOMETRIC ANALYSIS

A total of 1816 specimens of *Globigerinoides ruber albus* were classified and measured at the morphotype level. These specimens of *G. ruber albus* were assigned to the morphotypes cyclostoma (32.8%, 595/1816), platys (20.7%, 376/1816), kummerform (18.7%, 340/1816), normal (17.1%, 311/1816), elongatus cf. 1 (9.1%, 165/1816), elongatus pyramidical (1.0%, 19/1816), and twin (0.6 %, 10/1816).

Our first step of analysis was to evaluate the distributions of the morphometric measurements among *G. ruber albus* morphotypes. The morphotype elongatus pyramidical presented the highest median values for A_h, C_h, T_h, T_d, and t_w (Figure 3). Conversely, the smallest median values for A_h, T_h, T_d, and T_w were recorded for the morphotype cyclostoma, and the morphotype twin presented the smallest values for C_h and C_w (Figure 3). Except by C_h, the cyclostoma, elongatus cf. 1, and elongatus pyramidical morphotypes can be clearly distinguished. Specifically, elongatus pyramidical could be separates from all morphotypes using these morphometric variables. Furthermore, the kummerform morphotype can be clearly separated from the elongatus cf. 1 and elongatus pyramidical morphotypes by all the studied variables. On the contrary, it is evident that the platys and normal morphotypes cannot be separated for on the basis of single measured values.

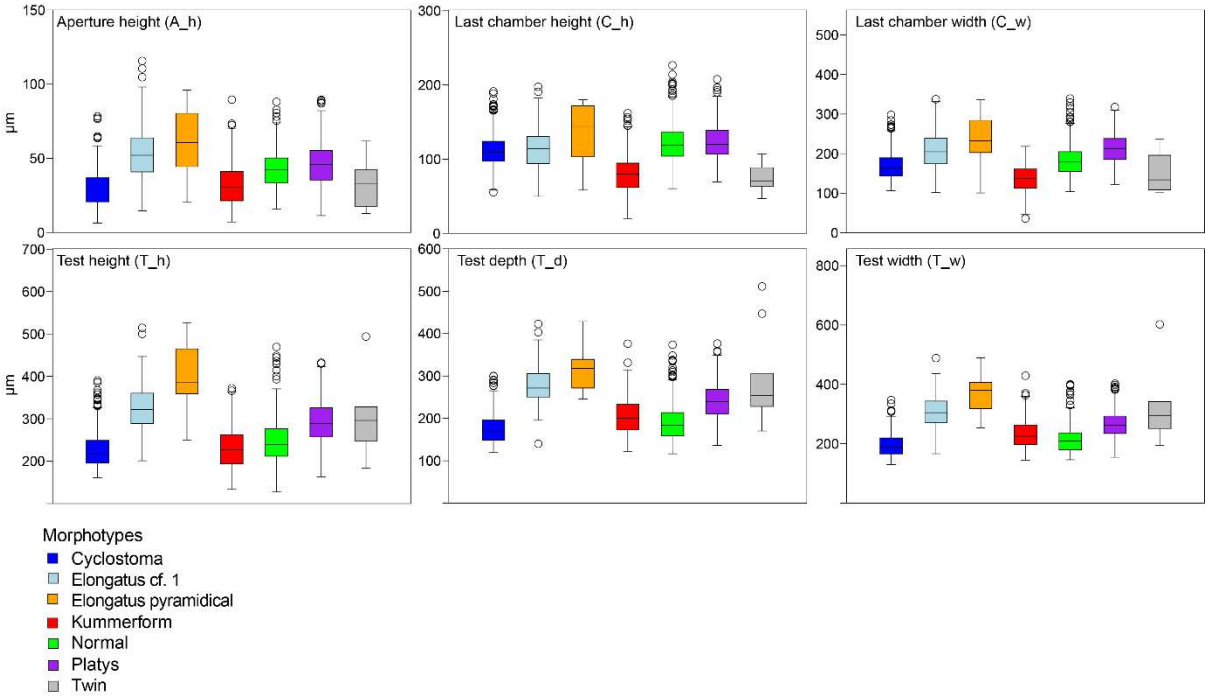

FIGURE 3- Log_{10}-scaled boxplots of individual morphometric parameters for each of the studied *G. ruber albus* morphotypes. Total numbers of specimens are: cyclostoma = 595, elongatus cf. 1= 165, elongatus pyramidical = 19, kummerform = 340, normal = 311, platys = 376, twin = 10.

The Mann-Whitney test demonstrates that most of the *G. ruber albus* morphotypes are significantly different from each other based on individual morphometric parameters, with only few exceptions (see Supplementary Table S2). The cluster analysis grouped the seven morphometric parameter as follows: (1) Test height (T_h) and test width (T_w); (2) test depth (T_d) and last chamber width (C_w); (3) last chamber height (C_h), aperture height (A_h) and aperture width (A_w) (Supplementary Figure S2).

Considering mostly ratios between parameters measured individually, scatter plots allowed to visually separate the cyclostoma, kummerform and platys morphotypes regarding T_h x C_h, C_h x C_w, T_h x T_w, T_hd x T_wd, CA_a x C_h, and A_hw x C_hw (Figure 4). These morphotypes can be clearly identified based on virtually all median values of individual parameters (Figure 3). The normal morphotype stood out regarding T_h x T_w, C_h x C_w, CA_a x C_h, and CA_a x A_hw (Figure 4). Considering median values of the measured parameters, normal specimens strongly overlap with the cyclostoma specimens, but both morphotypes can be differentiated based on A_h median values (Figure 3). The twin, elongatus cf.1 and elongatus pyramidical morphotypes did not show significant differentiation in the scatter plots.

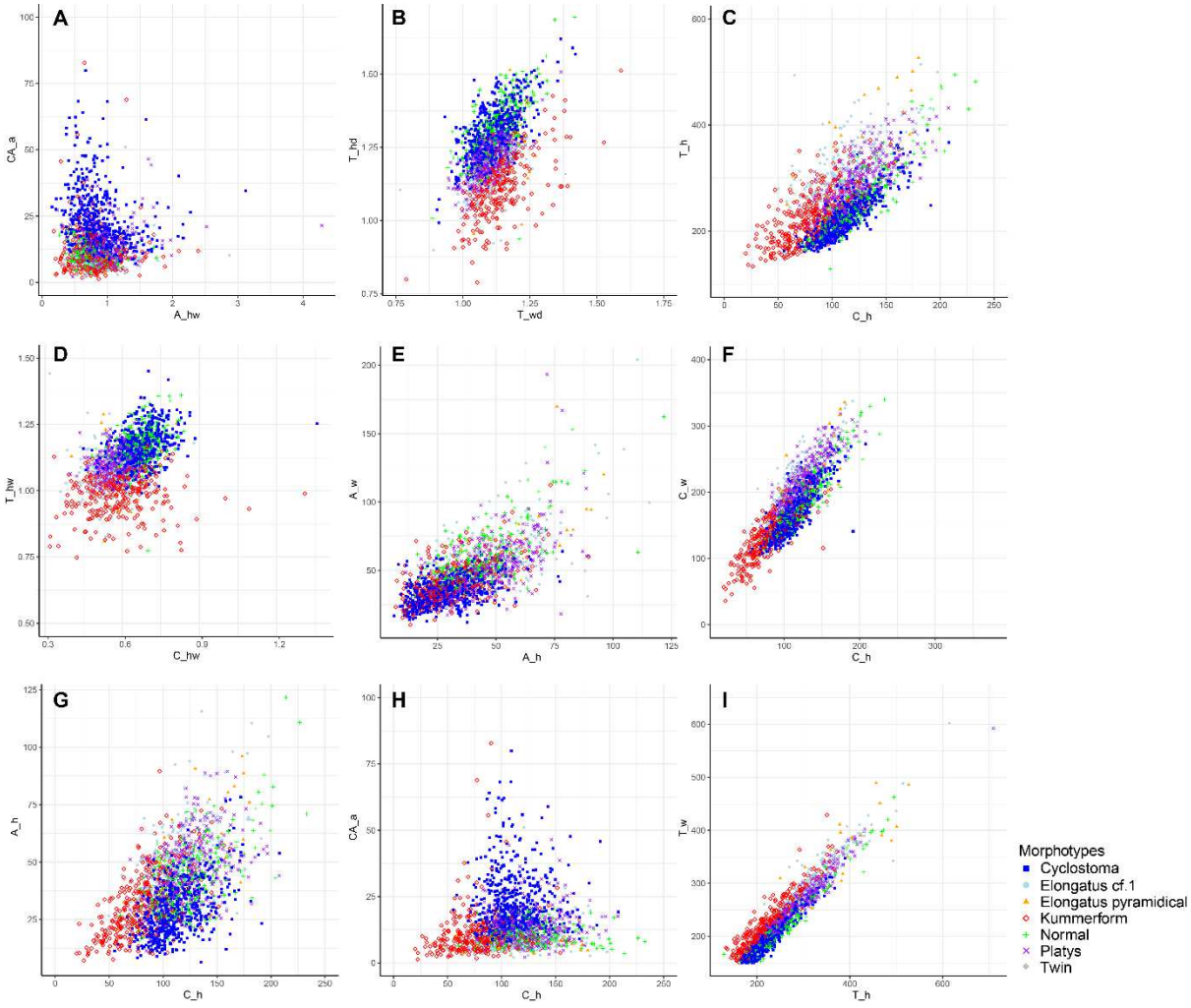

FIGURE 4- Scatterplots with measurements of all 1816 specimens indentified by morphotypes (except for a few outliers that plot outside the figured plot ranges). Parameters considered in the plots are: A_h (aperture height); A_w (aperture width); T_h (test height); T_w (test width); T_d (test depth); C_h (last chamber height); C_w (last chamber width); A_hw (aperture height/width ratio); C_hw (last chamber height/width ratio); CA_a (ratio between the area of the last chamber and the area of the aperture), T_wd (test width/depth ratio); T_hw (test height/width ratio); T_hd (test height/depth ratio). Dispersion plots were generated with the package ggplot2 (Wickham, 2016) in R environment (R Core Team, 2019).

4.2 STRATIGRAPHIC DISTRIBUTION OF MORPHOTYPES

The normal morphotype did not show significant changes in relative abundance throughout the studied glacial-interglacial cycles (MIS14-9; Figure 5). The cyclostoma morphotype presented its apexes of abundance within MIS 11 and MIS 13 (interglacial cycles), as opposed to the kummerform morphotype, which showed drops in abundance within MIS 11 and MIS 13 (Figure 5). The platys morphotype did not show significant oscillations, although its lowest percentage occurred within MIS 11 and MIS 13 interglacials (Figure 5). The morphotype elongatus cf. 1 presented low abundances in almost all samples, except for two peaks within MIS 13 (Figure 5). The elongatus pyramidical and twin morphotypes present percentages below 5% in all samples (Figure 5). The morphotype elongatus pyramidical had its abundance peaks within MIS 9, 11 and 13 interglacials, whereas the twin morphotype increased in abundance within MIS 10 and 12 glacials.

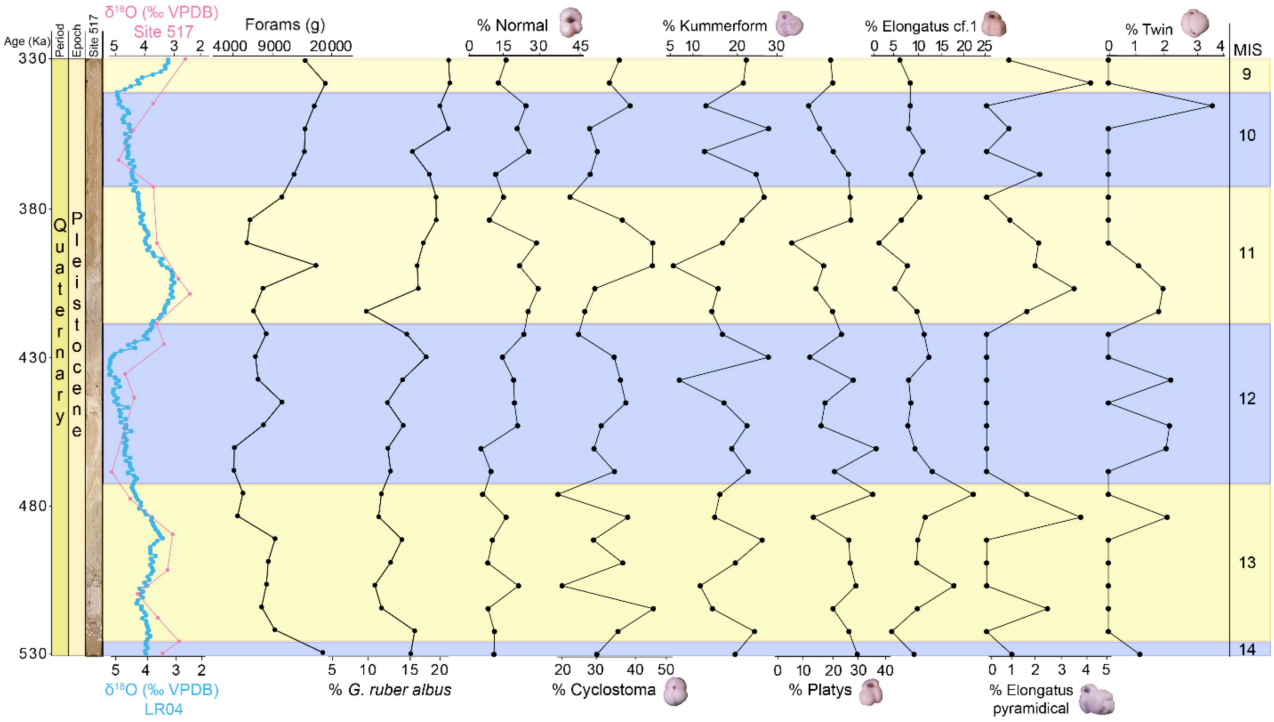

FIGURE 5- Distribution of *G. ruber albus* morphotypes along MIS 14 to 9 (late Pleistocene) at DSDP Site 517. We present estimates of the total amount of planktonic foraminifera per gram of sediment, as well as relative abundances of *G. ruber albus* and its identified morphotypes. For comparison, the global benthic foraminiferal $\delta^{18}O$ stack (LR04) of Lisiecki and Raymo (2005) is presented together with the benthic foraminiferal $\delta^{18}O$ record of Grazzini et al. (1983) for Site 517.

4.3 $\delta^{13}C$ AND $\delta^{18}O$ SIGNATURES OF G. RUBER ALBUS MORPHOTYPES

Globigerinoides ruber albus morphotypes show variability of $\delta^{18}O$ and, specially, $\delta^{13}C$ values during glacial and interglacial intervals (Figure 6). The cyclostoma morphotype had the lowest $\delta^{13}C$ values in four of the six glacial and interglacial isotopic stages (MIS 10, MIS 12, MIS 9 and MIS 11 respectively), and in the remaining two stages, MIS 14 and MIS 13, the second lowest $\delta^{13}C$ values (Figure 6). In glacial periods (MIS 10, MIS 12 and MIS 14; Figure 6), kummerforms and platys specimens showed the highest $\delta^{13}C$ values, followed by the normal morphotype, as is the case in interglacials, except for MIS 13, when the morphotype normal had the highest $\delta^{13}C$ value. The highest $\delta^{18}O$ values during glacial periods are recorded by the morphotype cyclostoma, whereas the overall lowest $\delta^{18}O$ values are presented by the normal morphotype. For interglacials, we could not identify any differentiation among the morphotypes based on $\delta^{18}O$ values.

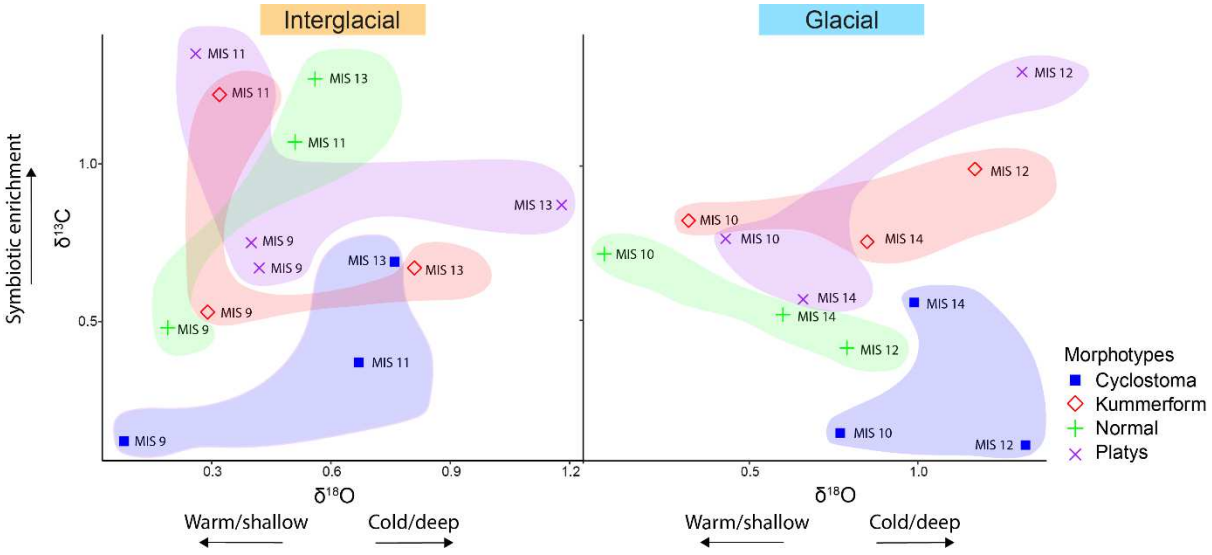

FIGURE 6- $\delta^{13}C$ and $\delta^{18}O$ values of the four most abundant *G. ruber albus* morphotypes for each MIS. For easier comparison, we present glacial and interglacial values separately. Note that each morphotype has well-defined isotopic niches in glacial periods, mostly along the $\delta^{13}C$ axis.

5 DISCUSSION

5.1 RELIABILITY OF IDENTIFYING *G. RUBER ALBUS* MORPHOTYPES

In our morphometric analysis we used both individual measured parameters, as well as morphometric ratios among several parameters. For instance, the size of the aperture, being observed in isolation, does not allow us to separate the studied morphotypes (Figure 4e), but when we compare aperture measurements with those of the last chamber, we were able to clearly separate morphotypes (Figure 4g, h). The most important parameters that allowed separating *G. ruber* morphotypes were C_w, C_h, A_w and A_h, confirming what we observed in the cluster analysis (Supplementary Figure S2).

The cyclostoma morphotype is easily distinguished in scatter plots (Figure 4a-d, f, i) and shows the smallest measurements in four of the six evaluated parameters (A_h, T_h, T_d and T_w; Figure 3). Considering the CA_a ratio (Figure 4a, h), which represents the relative proportion of the apertural area in relation to the last chamber (the closer to 1, the greater the aperture in relation to the last chamber), we can see that ~600 cyclostoma specimens show values between 12.5 and 80 (mostly between 12.5 and 50). These values evidence the main morphological characteristic of the cyclostoma morphotype: the small aperture in relation to the last chamber. We can see that the same pattern emerges when we look at the aperture height, since cyclostoma has the lowest values among all identified morphotypes (Figure 3). Our data, therefore, support classifying cyclostoma as a separate morphotype. However, studies on this morphotype are rare (e.g., Bonfardeci et al., 2018), and there are no molecular genetic data to infer whether cyclostoma in fact is a phenotypic variant of *G. ruber albus*, or whether it is a different species, as originally proposed by Galloway & Wissler (1927).

The normal morphotype (*G. ruber* sensu stricto of Wang, 2000) also presented some characteristic parameters and morphometric ratios (Figure 4a, b, f, h, i). This morphotype presents the median height of the last chamber higher than the other five morphotypes, being only lower than that of the elongatus pyramidical morphotype (Figure 3). When we observe the CA_a ratio (Figure 4a, h), all specimens of the normal morphotype are grouped between 25 and 0 (mostly between 0 and 12.5), evidencing its large aperture, one of its diagnostic characteristics. In the C_hw ratio (Figure 4d), referring to the degree of compression of the last chamber (the closer to 0, the more compressed the last chamber), most specimens of the normal morphotype exhibit values between 0.6 and 0.9, reinforcing the low degree of compression of its last chamber, which is also a striking feature of this morphotype. Kuroyanagi et al. (2008), showed that the normal morphotype is genetically distinct in up to 24% of its DNA from the sensu lato morphotype. The latter, in Kuroyanagi et al. (2008), includes the cyclostoma, elongatus cf. 1 and elongatus pyramidical morphotypes. The recent

molecular study of Aurahs et al. (2011) reinforced the significance of identifying the normal morphotype.

The kummerform morphotype was distinguished by almost all parameters and ratios (Figures 3, 4). Considering the height of the last chamber (C_h, Figure 4c, f, g, h), most kummerform specimens show values between 25 and 100 µm, relatively low when compared to the other morphotypes, which have values ranging from 75 to 200 µm. Kummerform specimens also present the shortest widths of the last chamber (C_w between 50 and 190 µm, Figure 4f). Regarding the degree of test compression (T_hw ratio; the smaller the number, the more compressed the test; Figure 4 d), kummerform specimens show the lowest values among all morphotypes, ranging from 0.75 to 1.10. The kummerform morphotype has lower median heights and widths of the last chamber than the other five morphotypes, but the medians for width and depth of the test are higher than those of the normal and cyclostoma morphotypes. Our measurements corroborate the main morphological characteristic of this morphotype, which is the abrupt decrease of the last chamber in relation to the previous ones. Kummerform is usually considered an informal morphotype (e.g., Numberger et al., 2009; Bonfardeci et al., 2018), as it refers to all specimens with a strong reduction in size of the last chamber, not only for *G.ruber albus,* but for other species as well, such as *Neogloboquadrina incompta* (Greco et al., 2020) and *Globigerina pachyderma* (Olson, 1973).

Specimens of the platys morphotype clustered with respect to some parameters (Figure 4b, c, d, f, h, i). Most specimens have low values, between 0.45 and 0.65, for the C_hw ratio (Figure 4 d), evidencing its main characteristic, which is the flattening of the last chamber. Considering individual parameters, it has values close to those of the normal morphotype with respect to the median height of the aperture and the median height of the last chamber (Figure 3, A_h and C_h), as well as median values higher than those of the normal morphotype for the width of the aperture, and height, width, and depth of the test (Figure 3, T_h, T_d and T_w). Therefore, our data allow to morphometrically differentiate the platys morphotype. Nevertheless, studies that identified this morphotype are rare (e.g., Numberger et al., 2009, Kontakiotis et al. 2017).

The morphotypes elongatus cf. 1, elongatus pyramidical and twin did not show significant differentiation in the scatter plots (Figure 4), probably because they are the least abundant morphotypes in all samples (165, 19 and 10 specimens, respectively). Considering median values, the elongatus pyramidical morphotype is distinguishable from the others, as it presents the highest values in all individual parameters, followed by the values of elongatus cf.1, mainly T_d (Figure 3), related to the elongation of the trochospiral whorl. Aurahs et al.

(2011), in their genetic study, suggested that *Globigerinoides elongatus* could be reintegrated as a distinct species. Morard et al. (2019), with ontogenetic and molecular genetic analyses, confirmed that *Globigerinoides elongatus* is in fact a separate species. However, both Aurahs et al. (2011) and Morard et al. (2019) analyzed platys and elongatus cf.1 specimens as being *G. elongatus*. Our results for the Mann-Whitney test show significant morphometric differences between platys and elongatus cf. 1 in five of the six parameters tested, pointing out similarity only for the last chamber width. We suggest that future genetic studies consider our new morphometric data to clarify whether the platys and elongatus cf. 1 should indeed be included under *G. elongatus*. Our data partially supports the interpretation of Aurahs et al. (2011) and Morard et al. (2019), that the morphotype defined here as elongatus cf.1 is in fact *G. elongatus*. Despite the large morphometric difference in the individual parameters (Figure 3), there are no genetic studies that identify the morphotype elongatus pyramidical as a separate species, as originally proposed by Van den Broeck (1876), who described it as *Globigerinoides pyramidalis*. Due to the similarity in the medians of individual morphometric parameters between elongatus pyramidical and elongatus cf. 1 (Figure 3), we suggest that elongatus pyramidical is a morphotype of the species *Globigerinoides elongatus* and not of *G. ruber albus.*

5.2 Ecological and environmental significance of *G. ruber albus* morphotypes

Changes in relative abundance of the morphotypes as well as their $\delta^{18}O$ and $\delta^{13}C$ signatures allow us to draw inferences about their (paleo)ecological preferences, as well as their environmental significances. Differentiations of $\delta^{18}O$ signatures were interpreted as evidencing preferences for slightly different depths within the upper water column, mainly during glacial periods. The low differentiation of $\delta^{18}O$ values among the studied *G. ruber* morphotypes in interglacial periods (Figure 6) probably reflects warm and homogeneous temperatures in the first 50 meters of water depth during these time intervals. We also interpreted differentiations of $\delta^{13}C$ values among the morphotypes as related to the occurrence of algal symbionts and/or particular paleoproductivity regimes.

At Site 517, the normal morphotype did not show significant variations in abundance between the glacial and interglacial periods, with only slightly higher relative abundances in interglacial periods, specifically in samples at 404 and 494 ka (Figure 5, MIS 11 and MIS 13, respectively). Wang (2000), studying South China Sea sediments, found significant

differences in the isotopic signals of oxygen and carbon between the s.s. (normal here) and s.l. (here platys, elongatus cf.1, elongatus pyramidical and cyclostoma) morphotypes. According to this author, the s.s. morphotype inhabits relatively shallow water depths (first 30 m), whereas the s.l. morphotype inhabits deeper water masses (below 30 m). Investigations on living foraminifera (Kuroyanagi & Kawahata, 2004) from the Japan Sea support this idea. Our $\delta^{18}O$ measurements revealed that the normal morphotype showed the lowest $\delta^{18}O$ values among all morphotypes for MIS 10, 12, 13 and 14 (Figure 6), further supporting a preference for warm surface waters.

The cyclostoma morphotype was more abundant in interglacial periods (Figure 5; MIS 11 and MIS13) at Site 517. This observation contrasts with the findings by Bonfardeci et al. (2018) for the North Atlantic, where cyclostoma was more abundant during glacial intervals (MIS 4 and MIS 2). Therefore, Bonfardeci et al. (2018) argued that the morphotype could be used as an indicator of relatively cool climate conditions. The $\delta^{18}O$ signal of cyclostoma during glacial periods at Site 517 (Figure 6, MIS 10, 12, and 14) is the highest among all morphotypes within each MIS, supporting a probable preference for relatively deep habitat (e.g., below 30 m) and cool waters.

The platys morphotype did not show significant variations in abundance along the studied interval of Site 517. This finding is in opposition with the pattern of increased platys abundances during glacial periods in the Mediterranean Sea (Numberger et al., 2009). Also, according to Numberger et al. (2009), the platys morphotype presented overall higher $\delta^{18}O$ values than the normal and *elongate* morphotypes (here as elongatus cf.1 and elongatus pyramidical) during MIS 12 to MIS 9. In our study, the platys morphotype indeed records higher $\delta^{18}O$ values than the normal morphotype in glacial periods (Figure 6; MIS 10, MIS 12 and MIS 14), but its $\delta^{18}O$ values were always lower than those of the cyclostoma morphotype. Therefore, we can infer a preference of the platys morphotype for an intermediate depth habitat, not as shallow and warm as that of the normal morphotype, but also not as deep and cold as that of cyclostoma.

The kummerform morphotype showed its highest relative abundances at Site 517 within MIS 10 and MIS 12 glacials and its lowest abundances within MIS 11 and MIS 13 interglacials (Figure 5), similar to the findings by Bonfardeci et al. (2018) in the North Atlantic Ocean for MIS 4 and MIS 2. Several authors have supported the hypothesis that the tiny final chamber of the kummerform morphotype is a response to environmental stress caused by cooling of the water column (Berger, 1969; Hecht & Savin, 1970, 1972; Hecht, 1974; Steinke et al., 2005). However, despite changes in relative abundance, kummerform

specimens are present in all samples from Site 517 (Figure 5). Hecht and Savin (1970, 1972) pointed out, based on stable isotope analyses, that kummerform specimens increased in abundance when sea surface temperatures (SSTs) were between 1° and 4.5 °C cooler than in intervals dominated by the normal morphotype at Sites from the Pacific and Atlantic oceans. In our work, the kummerform specimens present higher $\delta^{18}O$ values than the normal morphotype in all glacial periods (Figure 6; MIS 10, 12 and 14), but lower than those of the cyclostoma morphotype, similar to what was observed with the platys morphotype. These observations suggest an habitat depth preference of the kummerform morphotype comparable to that of the platys morphotype.

The twin morphotype was the least abundant throughout the studied interval at of Site 517, totaling only 10 specimens, and studies on this morphotype are scarce (e.g., Kontakiotis et al., 2017). A study using 40 core-top locations in the Mediterranean Sea (Antonarakou et al., 2018), correlated the appearance of the aberrant chamber in specimens of the twin morphotype to stressful environmental conditions, mainly hypersalinity, oligotrophy, low oxygenation, and water column stratification. Here we speculate that the formation of the aberrant chamber in twin specimens could be influenced by environmental stress associated with glacial conditions (e.g., changing trophic conditions and/or water column stratification), because they were present almost exclusively in glacial samples.

In the Mediterranean Sea (Numberger et al., 2009) the elongate morphotype (here referred to as elongatus cf. 1 and elongatus pyramidical) was more abundant in deglaciations and interglacials, and in the North Atlantic (Bonfardeci et al., 2018), the elongatus cf. 1 morphotype was more abundant in interglacials. Observations from these two locations are similar to our findings at Site 517. In our work, the morphotype elongatus cf. 1 presented low abundances and little variation along the succession, except for abundance peaks in the interglacial MIS 13 (Figure 5). Elongatus pyramidical was abundant in interglacial intervals (MIS 9, MIS 11 and MIS 13) and absent in the MIS 12 glacial (Figure 5), but its percentage did not exceed 5%. Bonfardeci et al. (2018) argued that the elongatus plexus could be used as a warm water indicator in the North Atlantic, but we cannot propose the same for the South Atlantic, due to the low amplitude variability of abundance changes.

We can observe a clear stratification of the morphotypes considering $\delta^{13}C$ values, mainly during glacial periods (Figure 6). *Globigerinoides ruber albus* carries photosynthetic dinoflagellate symbionts (Knight & Mantoura, 1985; Hemleben et al., 1989; Takagi et al., 2019), which influence calcite $\delta^{13}C$ values. Takagi et al. (2019) suggested that the depth of the habitat of the foraminiferal host is partially governed by the symbiont. Here in our study, the

cyclostoma morphotype has the highest $\delta^{18}O$ values, accompanied by the lowest $\delta^{13}C$ values, suggesting a relatively deep habitat, characterized by cool waters and low symbiont activity. Although the $\delta^{18}O$ signatures of kummerform and platys suggest a relatively deep habitat when compared with the normal morphotype, their high $\delta^{13}C$ values indicate high symbiont activity, followed by the normal morphotype, which probably lives in the shallower habitat.

6 CONCLUSIONS

Our study of the sedimentary succession comprising MIS 14 to 9 (530 to 330 ka) at Site 517 (South Atlantic Ocean) showed that the *G. ruber albus* morphotypes cyclostoma, normal, platys and kummerform present significant differences in morphometric measurements and ratios between individual measurements, occupying separate segments in morphospace. We also demonstrate that the most relevant morphological characters for the classification of *G. ruber albus* morphotypes are height and width of the last chamber, and height and width of the aperture.

Considering (paleo)ecological preferences, the cyclostoma morphotype was more abundant in interglacial periods and the kummerform morphotype was more abundant in the glacials in the South Atlantic subtropical gyre. We also identified characteristic $\delta^{18}O$ and $\delta^{13}C$ ranges for the four most abundant morphotypes (cyclostoma, normal, platys and kummerform). The cyclostoma morphotype presented the highest $\delta^{18}O$ values and the lowest $\delta^{13}C$ values, indicating a preference for deeper and colder waters with low symbiont activity. The normal morphotype showed the lowest $\delta^{18}O$ signature, evidencing its preference for shallow and warm waters, however its $\delta^{13}C$ values were lower than those of platys and kummerform, also suggesting reduced photosymbiont activity.

Due to the morphometric and isotopic differences between the *G. ruber albus* morphotypes, we suggest that future paleoceanographic studies consider identifying the normal, platys, kummerform and cyclostoma morphotypes, in addition to adopting a standard nomenclature. Because of morphometric patterns and recent genetic studies, we suggest that elongatus cf. 1 could be classified as a separate species, *Globigerinoides elongatus*, and that the elongatus pyramidical morphotype could be classified as a *G. elongatus* morphotype, due to the morphological similarities between them.

ACKNOWLEDGEMENTS

We thank the International Ocean Discovery Program (IODP) for providing the studied samples. The Brazilian National Council for Scientific and Technological Development is thanked for finantial support (CNPq grant 430253/2018-4). T. N. Z. received a scholarship by Coordination for the Improvement of Higher Education Personal (CAPES). All morphometric and stable isotope data are available as online supplementary material at the links (https://docs.google.com/spreadsheets/d/16OCBZi_J8tVt-b_z2F8t4B2HbyF7_0iAxx-Fe7Su9Dk/edit?usp=sharing and https://docs.google.com/spreadsheets/d/1gawDTb_Cgxq99GVt-ArNEeb1Ql5xHGvZ1Ss9UpnCBA4/edit?usp=sharing).

REFERENCES

Antonarakou, A., Kontakiotis, G., Zarkogiannis, S., Mortyn, P. G., Drinia, H., Koskeridou, E., and Anastasakis, G., 2018, Planktonic fora-miniferal abnormalities in coastal and open marine eastern Mediterranean environments: A natural stress monitoring approach inrecent and early Holocene marine systems: Journal of Marine Systems, v. 181, 63–78, doi: 10.1016/j.jmarsys.2018.02.004.

Aurahs, R., Treis, Y., Darling, K., and Kucera, M., 2011, A revised taxonomic and phylogenetic concept for the planktonic foraminifer species *Globigerinoides ruber* based on molecular and morphometric evidence: Marine Micropaleontology, v. 79, 1–14, doi: 10.1016/j.marmicro.2010.12.001.

Berger, W.H., 1969, Kummerform foraminifera as clues to oceanic environments: The American Association of Petroleum Geologists, v. 53, 706.

Boltovskoy, E., 1965, Los Foraminiferos Recientes: Eudeba, Buenos Aires, 510 p.

Bonfardeci, A., Caruso, A., Bartolini, A., Bassinot, F., and Blanc-Valleron, M.-M., 2018, Distribution and ecology of the *Globigerinoides ruber—Globigerinoides elongatus* morphotypes in the Azores region during the late Pleistocene-Holocene: Palaeogeography Palaeoclimatology Palaeoecology, v. 491, 92–111, doi: 10.1016/j.palaeo.2017.11.052.

Carter, A., Clemens, S., Kubota, Y., Holbourn, A., and Martin, A., 2017, Differing oxygen isotopic signals of two *Globigerinoides ruber* (white) morphotypes in the East China Sea: Implications for paleoenvironmental reconstructions: Marine Micropaleontology, v. 131, 1–9, doi: 10.1016/j.marmicro.2017.01.001.

Crivellari, S., Viana, P. J., Campos, M. C., Kuhnert, H., Barros, A., Cruz, F. W., and Chiessi, C. M., 2021, Development and characterization of a new in-house reference material for stable carbon and oxygen isotopes analyses: Journal of Analytical Atomic Spectrometry, v. 36, 1125–1134, doi: 10.1039/D1JA00030F.

Cushman, J.A., 1927, Some new genera of the foraminifera. Contr. Cushman Lab. Foramin. Res. Sharon Mass. 2, 77–81.

D'Orbigny, A. D., 1826, Tableau méthodique de la classe des Céphalopodes. Ann. Sci. Nat. Paris France Ser. I 7, 1–277.

Ericson, D. B., and Wollin, G., 1968, Pleistocene climates and chronology in deep-sea sediments: Science, v. 162, 1227–1234, doi: 10.1126/science.162.3859.1227.

Galloway, J. H., and Wissler, S. G., 1927, Pleistocene foraminífera from the Lomita Quarry, Palos Verdes Hills, California: Journal of Paleontology, v. 1, 35–87.

Grazzini, C. V., Grably, M., Pujol, C., and Duprat, J. M., 1983, Oxygen isotope stratigraphy and paleoclimatology of southwestern Atlantic Quaternary sediments (Rio Grande Rise) at Deep Sea Drilling Project Site 517, *in* Barker, P.F., et al. (eds.), Initial Reports of the Deep Sea Drilling Project: U.S. Govt. Printing Office, 72, 871–884, doi: 10.2973/dsdp.proc.72.143.1983.

Greco, M., Meilland, J., Zamelczyk, K., Rasmussen, T. L., and Kucera, M., 2020, The effect of an experimental decrease in salinity on the viability of the Subarctic planktonic foraminifera *Neogloboquadrina incompta*: Polar Research, v. 39, 1–8, doi: 10.33265/polar.v39.3842.

Hammer, Ø., Harper, D. A. T. and Ryan, P. D., 2001, PAST: Paleontological Statistics Software Package for education and data analysis: Palaeontologia Electronica, v. 4, 1–9.

Hecht, A. D., 1974, Intraspecific variation in recent populations of *Globigerinoides ruber* and *Globigerinoides trilobus* and their application to paleoenvironmental analysis: Journal of Paleontology, v. 48, 1217–1234.

Hecht, A. D., and Savin, S. M., 1970, Oxygen-18 studies of recent planktonic foraminifera: comparisons of phenotypes and of test parts: Science, v. 170, 69–71.

Hecht, A. D., and Savin, S. M., 1972, Phenotypic variation and oxygen isotope ratios in recent planktonic foraminifera: Journal of Foraminiferal Research, v. 2 (2), 55–67.

Hemleben, C., Spindler, M., and Anderson, O.R., 1989, Modern planktonic Foraminifera: Springer, Berlin, 363 p.

Hutson, W. H., 1980, The Agulhas Current During the Late Pleistocene: Analysis of Modern Faunal Analogs: Science, v. 207 (4426), 64–66, doi: 10.1126/ science.207.4426.64.

Jayan, A. K., Sijinkumar, A. V., and Nath, B. N., 2021, Paleoceanographic significance of *Globigerinoides ruber* (white) morphotypes from the Andaman Sea: Marine Micropaleontology, v. 165 (101996), 1–11, doi: 10.1016/j.marmicro.2021.101996.

Katz, M. E., Cramer, B. S., Franzese, A., Honisch, B., Miller, K. G., Rosenthal, Y., and Wright, J. D., 2010, Traditional and emerging geochemical proxies in foraminifera: Journal of Foraminiferal Research, v. 40 (2), 165–192, doi:10.2113/gsjfr.40.2.165.

Kawahata, H., 2005, Stable isotopic composition of two morphotypes of *Globigerinoides ruber* (white) in the subtropical gyre in the North Pacific: Paleontological Research, v. 9, 27–35.

Kemle-von-Mücke S., and Hemleben C., 1999, Planktic Foraminifera, *in* Boltovskoy, E., (ed) South Atlantic zooplankton: Backhuys Publishers, Leiden, p. 43–67.

Kennett, J. P., and Srinivasan, M. S., 1983, Neogene Planktonic Foraminifera: Hutchinson Ross Publishing Co., Stroudsburg, 265 p.

Knight, R., and Mantoura, R. F.C., 1985, Chlorophyll and carotenoid pigments in Foraminifera and their symbiotic algae: analysis by high performance liquid chromatography: Marine Ecology Progress Series, v. 23, 241–249.

Kontakiotis, G., Antonarakou, A., Mortyn, P. G., Drinia, H., Anastasakis, G., Zarkogiannis, S., and Mobius, J., 2017, Morphological recognition of *Globigerinoides ruber* morphotypes and their susceptibility to diagenetic alteration in the eastern Mediterranean Sea: Journal of Marine Systems, v. 174, 12– 24, doi: 10.1016/j.jmarsys.2017.05.005.

Kotov, S., and Pälike, H., 2018, QAnalySeries – a Cross-Platform Time Series Tuning and Analysis Tool: AGU Fall Meeting, Washington DC, doi: 10.1002/essoar.10500226.1.

Kuroyanagi, A., and Kawahata, H., 2004, Vertical distribution of living planktonic foraminifera in the seas around Japan: Marine Micropaleontology, v. 53, 173–196.

Kuroyanagi, A., Tsuchiya, M., Kawahata, H., and Kitazato, H., 2008, The occurrence of two genotypes of the planktonic foraminifer *Globigerinoides ruber* (white) and paleoenvironmental implications: Marine Micropaleontology, v. 68, 236–243.

Leipnitz, I. I., Silva, J. L. L., Leipnitz, B., Aguiar, E. S., Leão, C. J., Giovanoni, L., and Ferreira, F., 2005, Métodos para o trabalho com microfósseis e formas atuais, *in* Timm, L. L. and Cademartori, C. V. (eds.). Métodos de Estudo em Biologia: La Salle, Canoas, v. 2, p. 49–58.

Lin, H.-L., Wang, W.-C., and Hung, G.-W., 2004, Seasonal variation of planktonic foraminiferal isotopic composition from sediment traps in the South China Sea: Marine Micropaleontology, v. 53 (3–4), 447–460, doi:10.1016/j.marmicro.2004.08.004.

Lisiecki L. E., and Raymo M., E., 2005, A Pliocene-Pleistocene stack of 57 globally distributed benthic $d^{18}O$ records: Paleoceanography, v. 20, 1–17, doi:10.1029/2004PA001071.

Locarnini, R. A., Mishonov, O. K., Baranova, T. P., Boyer, M. M., Zweng, H. E., Garcia, J. R., Reagan, D., Seidov, K. W., Weathers, C. R., and Paver, I. V. S., 2019, World Ocean Atlas 2018, Temperature National Oceanic and Atmospheric Administration, Vol. 1 Temp. A. Mishonov, Tech. Ed. NOAA Atlas NESDIS 81, 1–52.

Löwemark, L., Hong, W. L., Yui, T. F., and Hung, G. W., 2005, A test of different factors influencing the isotopic signal of planktonic foraminifera in surface sediments from the northern South China Sea: Marine Micropaleontology, v. 55, 49–62, doi: S0377-8398(21)00037-2/rf0115.

Morard, R., Füllberg A, Brummer G-JA, Greco M, Jonkers L, Wizemann A, Weiner, A. K, Darling, K., Siccha, M., Ledevin, R., Kitazato, H., Garidel-Thoron, T., Vargas, C., and Kucera, M., 2019, Genetic and morphological divergence in the warm-water planktonic foraminifera genus *Globigerinoides*: PLoS One, v. 14(12), 1–30, doi: 10.1371/journal.pone.0225246.

Numberger, L., Hemleben, C., Hoffmann, R., Mackensen, A., Schulz, H., Wunderlich, J.M., and Kucera, M., 2009, Habitats, abundance patterns and isotopic signals of morphotype of the planktonic foraminifer *Globigerinoides ruber* (d'Orbigny) in the Eastern Mediterranean Sea since the marine isotopic stage 12: Marine Micropaleontology, v. 73, 90–104.

Olson, R. K. ,1973, What is a kummerform planktonic foraminifer?: Journal of Paleontology, v. 47, 327–329.

Pujol, C., 1983, Cenozoic planktonic foraminiferal biostratigraphy of the southwestern Atlantic (Rio Grande Rise): deep sea drilling project leg 72, *in* Barker, P. F., Carlson, R. L., Johnson, D. A., (eds.), Initial Reports of the Deep Sea Drilling Project: U.S. Govt. Printing Office, v. 72, 623– 673, doi: 10.2973/dsdp.proc.72.129.1983.

R Core Team, 2019, R: A Language and Environment for Statistical Computing: R Foundation for Statistical Computing, Vienna, https://www.R-project.org/

Schiebel, R., and Hemleben, C., 2017, Planktic foraminifers in the modern ocean: Springer, Berlin, 358 p.

Schlitzer, R., 2020, Ocean data view: ODV 5.2.1., http://odv.awi.de

Steinke, S., Chiu, H. Y., Yu, P. S., Shen, C. C., Löwemark, L., Mii, H. S., and Chen, M. T., 2005, Mg/Ca ratios of two *Globigerinoides ruber* (white) morphotypes: implications for reconstructing past tropical/subtropical surface water conditions: Geochemistry, Geophysics, Geosystems, v. 6, 1–12.

Stramma, L., and England, M., 1999, On the water masses and mean circulation of the South Atlantic Ocean: Journal of Geophysical Research Oceans, v. 104, 20863-20883.

Takagi H, Kimoto K, Fujiki T, Saito H, Schmidt C, Kucera M, and Moriya, K., 2019, Characterizing photosymbiosis in modern planktonic foraminifera: Biogeosciences discussion, v. 16, 3377–3396, doi: 10.5194/bg-2019-145.

Thirumalai, K., Richey, J. N., Quinn, T. M., and Poore, R. Z., 2014, *Globigerinoides ruber* morphotypes in the Gulf of Mexico: a test of null hypothesis: Scientific Reports, v. 4, 1–7, doi: S0377-8398(21)00037-2/rf0250.

Van den Broeck, E., 1876, Etude sur les Foraminiferes de la Barbade (Antilles): Socit belge de microscopie, An. 1, 55–152.

Wang, L. J., 2000, Isotopic signals in two morphotypes of *Globigerinoides ruber* (white) from the South China Sea: implications for monsoon climate change during the last glacial cycle: Palaeogeography, Palaeoclimatology, Palaeoecology, v. 161 (3–4), 381–394, https://doi.org/10.1016/S0031-0182(00)00094-8

Wickham, H., 2016, ggplot2: Elegant Graphics for Data Analysis: Springer-Verlag, New York, ISBN 978-3-319-24277-4, https://ggplot2.tidyverse.org.

4 CONCLUSÃO

Globigerinoides ruber albus foi a espécie mais abundante dentre as 27 reconhecidas no testemunho 517, o que atesta sua importância como espécie chave em estudos de reconstruções paleoceanográficas tropicais e subtropicais. Nosso estudo da sucessão sedimentar abrange MIS 14 a 9 (530 a 330 ka) mostrou que os morfotipos de *G. ruber* cyclostoma, normal, platys e kummerform apresentam diferenças significativas nas medições morfométricas e razões de medições individuais, ocupando segmentos separados no morfoespaço. Também demonstramos que os caracteres morfológicos mais relevantes para a classificação dos morfotipos *G. ruber albus* são altura e largura da última câmara e altura e largura da abertura.

Considerando as preferências (paleo)ecológicas, o morfotipo cyclostoma foi mais abundante em períodos interglaciais e o morfotipo kummerform foi mais abundante nas glaciais no giro subtropical do Atlântico Sul. Também identificamos características $\delta^{18}O$ e $\delta^{13}C$ para os quatro morfotipos mais abundantes (cyclostoma, normal, platys e kummerform). O morfotipo cyclostoma apresentou os valores mais altos de $\delta^{18}O$ e os menores valores $\delta^{13}C$, indicando preferência por águas mais profundas e frias com baixa atividade simbionte. O morfotipo normal mostrou os valores mais baixos de $\delta^{18}O$, evidenciando sua preferência por águas mais superficiais e quentes, porém seus valores de $\delta^{13}C$ eram inferiores aos de platys e kummerform, sugerindo também atividade fotossimbionte reduzida.

Os dados morfométricos reforçam a relevância da separação dos morfotipos normal, platys, kummerform e cyclostoma nos estudos paleoceanográficos futuros que pretendem usar a espécie *G. ruber albus* como *proxy*, corroborados pelas diferenças isotópicas entre os morfotipos. Há também a necessidade da adoção de uma nomenclatura padrão, pois vários estudos usam identificações diferentes para os mesmos morfotipos. Devido aos padrões morfométricos diferentes dos demais e estudos genéticos recentes, sugerimos que elongatus cf.1 seja classificado como uma espécie separada, *Globigerinoides elongatus*, e que o morfotipo elongatus pyramidical seja classificado como um morfotipo de *G. elongatus,* devido às semelhanças morfológicas entre eles.

REFERÊNCIAS

Aurahs, R., Treis, Y., Darling, K. & Kucera, M. 2011. A revised taxonomic and phylogenetic concept for the planktonic foraminifer species *Globigerinoides ruber* based on molecular and morphometric evidence. Marine Micropaleontology. 79: 1-14

Aze, T., Ezard, T. H. G., Purvis, A., Stewart, D., Coxall, H. K., Wade, B. S. & Pearson, P. N. 2011. A phylogeny of Cenozoic macroperforate planktonic foraminifera from fossil data. Biological Reviews. 86: 900-927.

Bé, A.W.H., Hemleben, C., Anderson, O.R., Spindler, M., Hacunda J, Tuntivate-Choy S 1977. Laboratory and field observations of living planktonic Foraminifera. Micropaleontology 23:155–179

Berger, W.H., 1969. Kummerform foraminifera as clues to oceanic environments. The American Association of Petroleum Geologists 53, 706.

Boltovskoy, E. 1965. Los Foraminiferos Recientes. Buenos Aires: Eudeba, 1965.

Bonfardeci, A., Caruso, A., Bartolini, A., Bassinot, F., & Blanc-Valleron, M.-M. 2018. Distribution and ecology of the *Globigerinoides ruber—Globigerinoides elongatus* morphotypes in the Azores region during the late Pleistocene-Holocene. Palaeogeography Palaeoclimatology Palaeoecology, 491, 92–111. doi: 10.1016/j.palaeo.2017.11.052

Cushman, J.A. 1914. A monograph of the foraminifera of the North Pacific Ocean. Part 4. Chilostomellidae, Globigerinidae, Nummulitidae. Washington Smithsonian. Inst. U.S. Nation Mus. Bull. 71, 1–46.

Cushman, J.A. 1927. Some new genera of the foraminifera. Contr. Cushman Lab. Foramin. Res. Sharon Mass. 2, 77–81.

D'Orbigny, A. D. 1826. Tableau méthodique de la classe des Céphalopodes. Ann. Sci. Nat. Paris France Ser. I 7, 1–277.

D'Orbigny, A. D. 1839. Foraminiferes. In, de la Sagra, R. (ed.) Histoire physique et naturelle de l'Ile de Cuba. A. Bertrand, Paris, France 1-224.

Ericson, D. B. & Wollin, G. 1968. Pleistocene climates and chronology in deep-sea sediments. Science, 162, 1227-1234. doi: 10.1126/science.162.3859.1227

Galloway, J.H., Wissler, S.G. 1927. Pleistocene foraminífera from the Lomita Quarry, Palos Verdes Hills, California. J. Paleontol. 1, 35–87.

Ganssen, G., Peeters, F. J. C., Metcalfe, B., Anand, P., Jung, S. J. A., Kroon, D., Brummer, G.-J. A. 2010. Quantifying sea surface temperature ranges of the Arabian Sea for the past 20 000 years. Clim. Past Discuss. 6, 2795–2814.

Hecht, A.D., Savin, S.M. 1970. Oxygen-18 studies of recent planktonic foraminifera: comparisons of phenotypes and of test parts. Science 170, 69–71.

Hemleben, C., Spindler, M., Anderson, O.R. 1989. Modern planktonic Foraminifera. Springer, Berlin

Hutson, W. H. 1980. The Agulhas Current During the Late Pleistocene: Analysis of Modern Faunal Analogs. Science, 207 (4426), 64-66. doi: 10.1126/science.207.4426.64.

Katz, M. E., Cramer, B. S., Franzese, A., Honisch, B., Miller, K. G., Rosenthal, Y., Wright, J. D. 2010. Traditional and emerging geochemical proxies in foraminifera. The Journal of Foraminiferal Research, 40(2), 165–192. doi:10.2113/gsjfr.40.2.165

Kawahata, H. 2005. Stable isotopic composition of two morphotypes of *Globigerinoides ruber* (white) in the subtropical gyre in the north Pacific. Paleontological Research 9 (1), 27–35.

Kemle-von-Mücke, S., Hemleben, C. 1999. Planktic Foraminifera. In: Boltovskoy, E. (ed) South Atlantic zooplankton. Backhuys Publishers, Leiden, pp 43–67

Kennett, J. P. & Srinivasan, M. S. 1983. Neogene Planktonic Foraminifera. Hutchinson Ross Publishing Co., Stroudsburg, Pennsylvania. 1-265.

Kontakiotis, G., Antonarakou, A., Mortyn, P. G., Drinia, H., Anastasakis, G., Zarkogiannis, S., Mobius, J. 2017. Morphological recognition of *Globigerinoides ruber* morphotypes and their susceptibility to diagenetic alteration in the eastern Mediterranean Sea. Journal of Marine Systems, 174, 12– 24. doi: 10.1016/j.jmarsys.2017.05.005

Kucera, M. 2007. Planktonic Foraminifera as Tracers of Past Oceanic Environments. In: Hillaire-Marcel, C.; de Vernal, A. Proxies in Late Cenozoic paleoceanography, vol. 1, Developments in Marine Geology. Amsterdam, Boston Elsevier, 213–262. doi:10.1016/s1572-5480(07)01011-1.

Kuroyanagi, A., Tsuchiya, M., Kawahata, H., Kitazato, H. 2008. The occurrence of two genotypes of the planktonic foraminifer *Globigerinoides ruber* (white) and paleoenvironmental implications. Marine Micropaleontology 68, (236–243).

Lin, H.L., Wang, W.C., Hung, G.W. 2004. Seasonal variation of planktonic foraminiferal isotopic composition from sediment traps in the South China Sea. Marine Micropaleontology 53 (3–4), 447–460

Lisiecki L.E., Raymo M., E. 2005. A Pliocene-Pleistocene stack of 57 globally distributed benthic d18O records. Paleoceanography. doi:10.1029/2004PA001071

Locarnini, R.A., A.V. Mishonov, O.K. Baranova, T.P. Boyer, M.M. Zweng, H.E. Garcia, J.R. Reagan, D. Seidov, K.W. Weathers, C.R. Paver, and I. V. S. 2019. World Ocean Atlas 2018, Volume 1: Temperature NOAA Atlas NESDIS 81 WORLD OCEAN ATLAS 2018 Volume 1: Temperature National Oceanic and Atmospheric Administration. World Ocean Atlas 2018, Vol. 1 Temp. A. Mishonov, Tech. Ed. NOAA Atlas NESDIS 81, 52pp. 1, 52

LoDico, J. M., Flower, B. P., Quinn, T. M. 2006. Subcentennial-scale climatic and hydrologic variability in the Gulf of Mexico during the early Holocene. Paleoceanography 21, PA3015.

Löwemark, L., Hong, W.L., Yui, T.F., Hung, G.W. 2005. A test of different factors influencing the isotopic signal of planktonic foraminifera in surface sediments from the northern South China Sea. Marine Micropaleontology 55/1–2, 49–62.

Morard, R., Füllberg, A., Brummer, G-J.A., Greco, M., Jonkers, L., Wizemann, A., Weiner, A. K. M., Darling, K., Siccha, M., Ledevin, R., Kitazato, H., Garidel-Thoron, T., Vargas, C., Kucera, M. 2019. Genetic and morphological divergence in the warm-water planktonic foraminifera genus *Globigerinoides.* PLoS One. 14(12): 1-30. doi: 10.1371/journal.pone.0225246

Numberger, L., Hemleben, C., Hoffmann, R., Mackensen, A., Schulz, H., Wunderlich, J.M., Kucera, M. 2009. Habitats, abundance patterns and isotopic signals of morphotype of the planktonic foraminifer *Globigerinoides ruber* (d'Orbigny) in the Eastern Mediterranean Sea since the marine isotopic stage 12. Mar. Micropaleontol. 73, 90–104

Robbins, L.L., Healy-Williams, N. 1991. Toward a classification of planktonic-foraminifera based on biochemical, geochemical, and morphological criteria. Journal of Foraminiferal Research 21 (2), 159–167.

Rohling, E., Sprovieri, M., Cane, T., Casford, J.S.L., Cooke, S., Bouloubassi, I., Emeis, K.C., Schiebel, R., Rogerson, M., Hayes, A., Jorissen, F.J., Kroon, D. 2004. Reconstructing past planktic foraminiferal habitats using stable isotope data: a case history for Mediterranean sapropel S5. Marine Micropaleontology 50, 89–123.

Sadekov, A., Eggins, S, De Deckker P., Kroon, D. 2008. Uncertainties in seawater thermometry deriving from intratest and intertest Mg/Ca variability in *Globigerinoides ruber* Paleoceanography, 23, doi: 10.1029/2007PA001452

Schiebel, R., Hemleben, C. 2017. Planktic foraminifers in the modern ocean. Springer, Berlin, Heidelberg

Schiebel, R., Zeltner, A., Treppke, U.F., Waniek, J.J., Bollmann, J., Rixen, T. et al. 2004. Distribution of diatoms, coccolithophores and planktic foraminifers along atrophic gradient during SW monsoon in the Arabian Sea. Marine Micropaleontol., 51, 345– 371.

Steinke, S., Chiu, H.Y., Yu, P.S., Shen, C.C., Löwemark, L., Mii, H.S., Chen, M.T. 2005. Mg/Ca ratios of two *Globigerinoides ruber* (white) morphotypes: implications for reconstructing past tropical/subtropical surface water conditions. Geochemistry, Geophysics, Geosystems 6.

Thirumalai, K., Richey, J.N., Quinn, T. M; Poore, R. Z. 2014. *Globigerinoides ruber* morphotypes in the Gulf of Mexico: a test of null hypothesis Sci. Rep., 4, p. 6018, doi: 10.1038/srep06018

Thompson, P. R., Be, A. W. H., Duplessy, J. C., Shackleton, N. J. 1979. Disappearance of white pigmented *Globigerinoides ruber* at 120, 000 yr BP in the Indian and Pacific Oceans. Nature. 280: 554-558.

Van den Broeck, E. 1876. Etude sur les Foraminiferes de la Barbade (Antilles). Soc. Belge Microsc. An. 1, 55–152.

Wang, L.J. 2000. Isotopic signals in two morphotypes of *Globigerinoides ruber* (white) from the South China Sea: implications for monsoon climate change during the last glacial cycle. Palaeogeography, Palaeoclimatology, Palaeoecology 161 (3–4), 381–394. doi: 10.1016/S0031-0182(00)00094-8

Weldeab, S., Lea, D. W., Oberha¨nsli, H. & Schneider, R. R. 2014. Links between southwestern tropical Indian Ocean SST and precipitation over southeastern Africa over the last 17 kyr. Palaeogeogr. Palaeoclimatol. Palaeoecol. 410, 1–13.

Supplementary material:

ASSESSING THE SIGNIFICANCE OF IDENTIFYING *GLOBIGERINOIDES RUBER ALBUS* MORPHOTYPES IN THE SOUTH ATLANTIC SUBTROPICAL GYRE DURING THE LATE PLEISTOCENE

By: Tamires Nunes Zardin, Karlos G. D. Kochhann, Jorge Villegas. Martín, Guilherme Krahl, Gerson Fauth

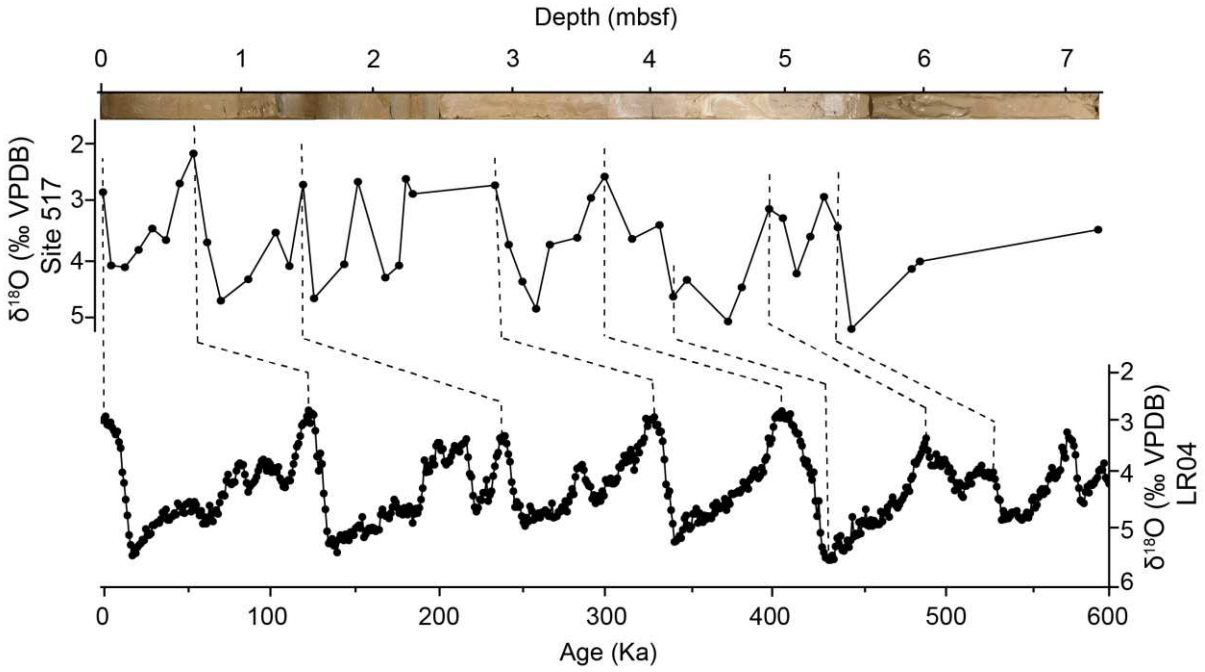

Supplementary Figure S1- Age model for DSDP Site 511. We correlated the benthic foraminiferal $\delta^{18}O$ record of Grazzini et al. (1983) with the global stack LR04 of Lisieck and Raymo (2005).

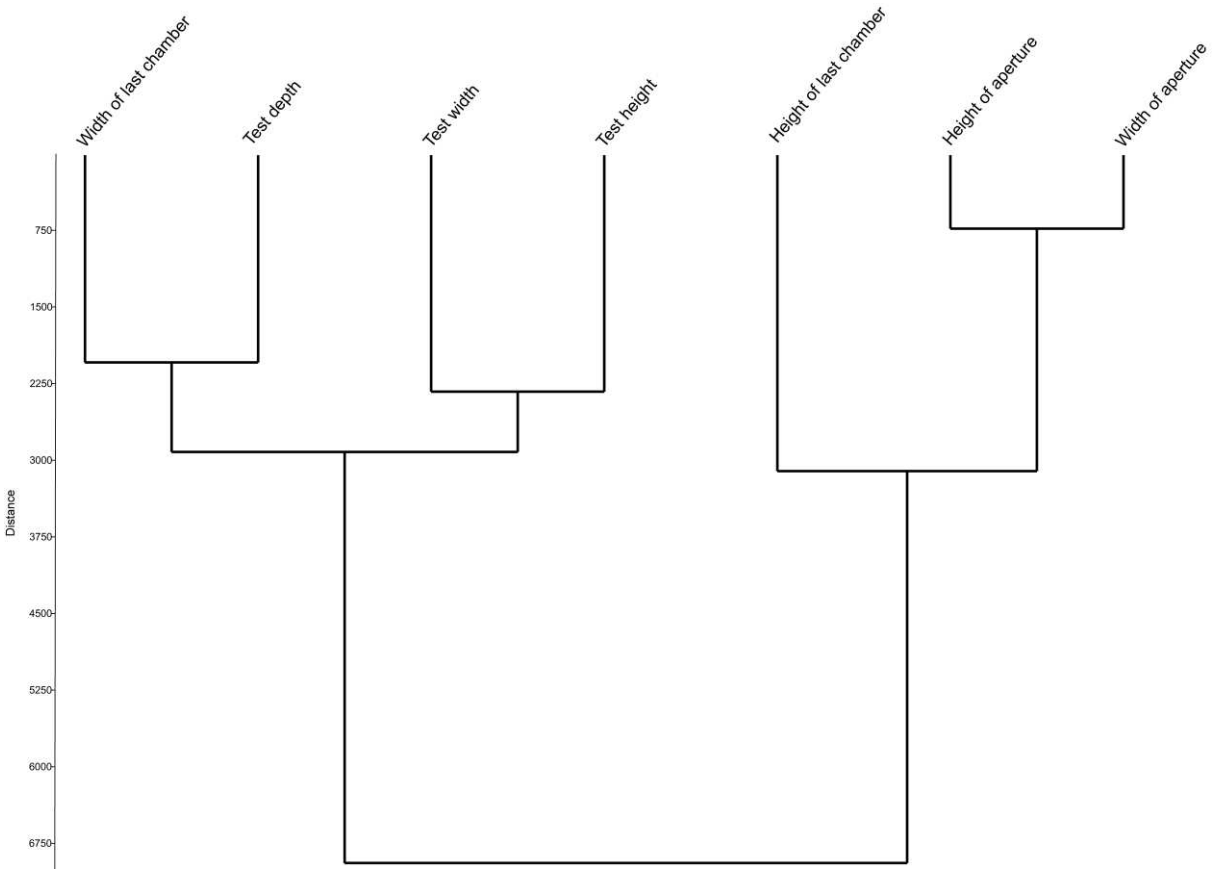

Supplementary Figure S2- Cluster analysis of the seven parameters measured on *G. ruber albus* morphotypes. Parameters that vary in similar ways among morphotypes are grouped closer together.

Supplementary Table S1- Age to depth tie points used in the age model for DSDP Site 517.

$\delta^{18}O$ Site 517	Level in m	Age
2,8	0.04	0
2,13	0.7	123
2,67	1.5	240
2,68	2.9	330
2,53	3.7	406
4,61	4.2	431
3,09	4.9	490
3,41	5.4	530

Supplementary Table S2- Results of the Mann-Whitney tests. All values in bold suggest significant differences among morphotypes.

Table S2.1. Result of Mann Whitney test comparing all morphotypes based on the height of the last chamber.

	cyclostoma	Elongatus cf.1	elongatus pyramidical	kummerform	normal	platys	twin
cyclostoma		p=0.28	**p=0.003**	**p <0.0001**	**p <0.0001**	**p <0.0001**	**p <0.0001**
Elongatus cf.1	p=0.28		**p=0.02**	**p <0.0001**	**p=0.007**	**p=0.0004**	**p <0.0001**
elongatus pyramidical	**p=0.003**	**p=0.02**		**p <0.0001**	p=0.08	p=0.09	**p=0.0007**
kummerform	**p <0.0001**	**p <0.0001**	**p <0.0001**		**p <0.0001**	**p <0.0001**	p=0.40
normal	**p <0.0001**	**p=0.007**	p=0.08	**p <0.0001**		p=0.25	**p <0.0001**
platys	**p <0.0001**	**p=0.0004**	p=0.09	**p <0.0001**	p=0.25		**p <0.0001**
twin	**p <0.0001**	**p <0.0001**	**p=0.0007**	p=0.40	**p <0.0001**	**p <0.0001**	

Table S2.2. Result of Mann Whitney test comparing all morphotypes for test height.

	cyclostoma	Elongatus cf.1	elongatus pyramidical	kummerform	normal	platys	twin
cyclostoma		**p <0.0001**	**p <0.0001**	p=0.21	**p <0.0001**	**p <0.0001**	**p=0.0007**
Elongatus cf.1	**p <0.0001**		**p <0.0001**	**p <0.0001**	**p <0.0001**	**p <0.0001**	p=0.21
elongatus pyramidical	**p <0.0001**	**p <0.0001**		**p <0.0001**	**p <0.0001**	**p <0.0001**	**p=0.02**
kummerform	p=0.21	**p <0.0001**	**p <0.0001**		**p <0.0001**	**p <0.0001**	**p=0.003**
normal	**p <0.0001**	**p <0.0001**	**p <0.0001**	**p <0.0001**		**p <0.0001**	**p=0.02**
platys	**p <0.0001**	**p <0.0001**	**p <0.0001**	**p <0.0001**	**p <0.0001**		p=0.83
twin	**p=0.0007**	p=0.21	**p=0.02**	**p=0.003**	**p=0.02**	p=0.83	

Table S2.3. Result of Mann Whitney test comparing all morphotypes for test width.

	cyclostoma	Elongatus cf.1	elongatus pyramidical	kummerform	normal	platys	twin
cyclostoma		**p <0.0001**	**p <0.0001**	**p <0.0001**	**p <0.0001**	**p <0.0001**	**p <0.0001**
Elongatus cf.1	**p <0.0001**		**p <0.0001**	**p <0.0001**	**p <0.0001**	**p <0.0001**	p=0.39
elongatus pyramidical	**p <0.0001**	**p <0.0001**		**p <0.0001**	**p <0.0001**	**p <0.0001**	**p=0.02**
kummerform	**p <0.0001**	**p <0.0001**	**p <0.0001**		**p <0.0001**	**p <0.0001**	**p=0.002**
normal	**p <0.0001**	**p <0.0001**	**p <0.0001**	**p <0.0001**		**p <0.0001**	**p=0.0003**
platys	**p <0.0001**	**p <0.0001**	**p <0.0001**	**p <0.0001**	**p <0.0001**		p=0.16
twin	**p <0.0001**	p=0.39	**p=0.02**	**p=0.002**	**p=0.0003**	p=0.16	

Table S2.4. Result of Mann Whitney test comparing all morphotypes for last chamber width.

	cyclostoma	Elongatus cf.1	elongatus pyramidical	kummerform	normal	platys	twin
cyclostoma		**p <0.0001**	**p <0.0001**	**p <0.0001**	**p <0.0001**	**p <0.0001**	**p=0.045**
Elongatus cf.1	**p <0.0001**		**p=0.06061**	**p <0.0001**	**p <0.0001**	p=0.14	**p=0.001**
elongatus pyramidical	**p <0.0001**	p=0.06		**p <0.0001**	**p=0.0001**	p=0.09	**p=0.004**
kummerform	**p <0.0001**	**p <0.0001**	**p <0.0001**		**p <0.0001**	**p <0.0001**	p=0.77
normal	**p <0.0001**	**p <0.0001**	**p=0.0002**	**p <0.0001**		**p <0.0001**	**p=0.01**
platys	**p <0.0001**	p=0.14	p=0.09	**p <0.0001**	**p <0.0001**		**p=0.0002**
twin	**p=0.045**	**p=0.001**	**p=0.004**	p=0.77	**p=0.01**	**p=0.0002**	

Table S2.5. Result of Mann Whitney test comparing all morphotypes for aperture height.

	cyclostoma	Elongatus cf.1	elongatus pyramidical	kummerform	normal	platys	twin
cyclostoma		**p <0.0001**	**p <0.0001**	**p=0.01098**	**p <0.0001**	**p <0.0001**	p=0.85
Elongatus cf.1	**p <0.0001**		p=0.09	**p <0.0001**	**p <0.0001**	**p <0.0001**	**p=0.0006**
elongatus pyramidical	**p <0.0001**	p=0.09		**p <0.0001**	**p=0.0002**	**p=0.002**	**p=0.001**
kummerform	**p=0.01098**	**p <0.0001**	**p <0.0001**		**p <0.0001**	**p <0.0001**	**p=0.7693**
normal	**p <0.0001**	**p <0.0001**	**p=0.0002**	**p <0.0001**		**p=0.0002**	**p=0.01**
platys	**p <0.0001**	**p <0.0001**	**p=0.002**	**p <0.0001**	**p=0.0002**		**p=0.003**
twin	p=0.85	**p=0.0006**	**p=0.001**	p=0.77	p=0.01	**p=0.003**	

Table S2.6. Result of Mann Whitney test comparing all morphotypes for test depth.

	cyclostoma	Elongatus cf.1	**elongatus pyramidical**	kummerform	normal	platys	twin
cyclostoma		**p <0.0001**	**p <0.0001**	**p <0.0001**	**p <0.0001**	**p <0.0001**	**p <0.0001**
Elongatus cf.1	**p <0.0001**		**p <0.001**	**p <0.0001**	**p <0.0001**	**p <0.0001**	p=0.38
elongatus pyramidical	**p <0.0001**	**p <0.001**		**p <0.0001**	**p <0.0001**	**p <0.0001**	p=0.05
kummerform	**p <0.0001**	**p <0.0001**	**p <0.0001**		**p <0.0001**	**p <0.0001**	**p=0.002**
normal	**p <0.0001**	**p <0.0001**	**p <0.0001**	**p <0.0001**		**p <0.0001**	**p=0.00028**
platys	**p <0.0001**	**p <0.0001**	**p <0.0001**	**p <0.0001**	**p <0.0001**		p=0.26
twin	**p <0.0001**	p=0.38	p=0.05	**p=0.002**	**p=0.0003**	p=0.26	